eLife

Reviewed Preprint
v1 • May 22, 2026
Not revised

For correspondence:
heyulong@suda.edu.cn

# Equal contribution

Competing interests: No competing interests declared

Funding: See page 20

Reviewing editor: Maike Frye, University Medical Center Hamburg-Eppendorf, Germany

Endocardial TIE1 synergizes with TIE2 to regulate the atrial internal muscular network assembly

Kai Ding[1,#], Beibei Xu[1,#], Xinhao Yu[1], Xiwen Jia[1], Taotao Li[1], Xin Shen[1], Junda Li[1], Xudong Cao[1], Yahui Liu[1], Zhen Zhang[2,3], Yulong He[1]

[1]Cyrus Tang Hematology Center, Collaborative Innovation Center of Hematology, National Clinical Research Center for Hematologic Diseases, State Key Laboratory of Radiation Medicine and Protection, Cam-Su Genomic Resources Center, Suzhou Medical College of Soochow University, Suzhou, China • [2]Pediatric Translational Medicine Institute and Pediatric Congenital Heart Disease Institute, Shanghai Children's Medical Center, Shanghai Jiao Tong University School of Medicine, Shanghai, China • [3]Shanghai Collaborative Innovative Center of Intelligent Medical Device and Active Health, Shanghai University of Medicine & Health Sciences, Shanghai, China

eLife Assessment

This study reports the relative importance of Tie1 and Tie2 signaling for atrial versus ventricular trabeculation. It is an **important** study and is one of the few works to date that have carefully and simultaneously analyzed these two processes. In line with a previous study in zebrafish, the authors demonstrate key differences between atrial and ventricular trabeculation. While the imaging and quantitative data were conducted with **solid** and validated methodology throughout the manuscript, the work would benefit from more rigourous approaches where Tie1/2 signaling is disrupted prior to the onset of atrial/ventricular trabeculation, to allow for a more direct comparison.

https://doi.org/10.7554/eLife.111156.1.sa4

Abstract

Atrial cardiomyopathy is characterized by altered atrial structures and the genetic basis underlying the disorders remains inadequately explored. TIE1 variants or loss of function mutations were reported in a subset of lymphedema patients, and it is unknown whether the patients have also cardiac defects in addition to the lymphatic abnormality. We show in this study that endothelial *Tie1* and *Tek* are highly expressed in endocardial cells of atria by the single cell RNA-seq analysis. TIE1 deficiency led to the disruption of atrial morphogenesis with minor defects in the ventricles. The bulk RNA-seq analysis of hearts at the four-chambered stage revealed that gene transcripts related to endothelial cell development and cardiac trabeculation were reduced in the *Tie1* mutant mice compared with littermate controls. This was further confirmed by the RNA-seq analysis of atria and ventricles separately, showing more trabecular genes downregulated in the atria including *Tek*, upon the loss of *Tie1*. Consistent with the scRNA-seq data, we found that *Tie1* and *Tek* transcripts were higher in atria than in ventricles. Furthermore, the endothelial deletion of *Tek* resulted in the defective formation of cardiac trabeculae, particularly in atria. Consistently, the loss of *Tie1* combined with one null allele of *Tek* disrupted both atrial and ventricular trabeculation. Surprisingly, defects with the atrial chamber morphogenesis were already detectable 48 hours later upon the induced endothelial loss of *Tie1* plus the *Tek* heterozygous deletion, implying a critical role of endocardium in the organization of the atrial internal muscular network. The synergy of TIE1 and TIE2 in the remodeling of atrial trabeculae was further confirmed at the postnatal stage, while TIE1 insufficiency alone had no

obvious effect. Together, findings from this study imply that TIE1 is differentially required for the atrial and ventricular development and acts in synergy with TIE2 to regulate the endocardial cell-coordinated atrial internal muscular network assembly.

Introduction

The endocardium, as a specialized type of endothelial cells (EC) lining the cardiac lumen, plays an important role in vertebrate heart morphogenesis [1,2]. Cardiac trabeculation relies on the coordinated interaction of endocardium and myocardium [3,4]. The endocardium senses mechanical forces and provides signals for the myocardial morphogenesis [5]. When endocardial cells fail to form buds, the assembly and extension process of trabeculae are disrupted [2,6]. Defective trabecular formation could lead to embryonic lethality or congenital heart disease [7–9]. Cell lineage studies have also shown that the endocardium is an important source of the coronary vascular endothelial cells, and gives rise to most mesenchymal cells that constitute the cardiac cushions and subsequently contribute to the heart valves [10]. Atrial internal muscular networks, mainly pectinate muscles running in an anterolateral direction, are found on the anterior surface of both right and left atrial walls and corresponding auricles. In contrast to the better understanding of ventricular trabecula morphogenesis, the dynamic process and regulatory networks of atrial trabeculation are inadequately elucidated. Likewise, the atrial cardiomyopathy is characterized by altered atrial structure as well as function, and pathological mechanisms underlying the disorders are largely unknown.

Cardiac morphogenesis is a complex process involving multiple pathways to orchestrate the reciprocal paracrine signaling between the endocardial and other cardiac cells. Specifically, myocardial VEGFA activates VEGFR2 signaling for coronary vascular growth and also participate in the regulation of cardiac trabeculation [11]. Endocardial cell-derived NRG1 regulates myocardium development via its receptors ERBB2/4 in cardiomyocytes. Mice null for *Nrg1* or its receptors display hypoplastic ventricular wall lacking normal trabeculation [12]. The aberrant NOTCH1 signaling was found to disrupt the heart morphogenesis [13,14]. NRG1 has been show to regulate VEGFA expression in the myocardium, and VEGFA-VEGFR2 signaling is required for the NOTCH1 pathway restriction in endocardium during trabeculation. NOTCH1 signaling was shown to promote extracellular matrix (ECM) degradation during the formation of endocardial projections while NRG1 promoted myocardial ECM synthesis for trabecular rearrangement during the process of cardiac trabeculation [15]. It has recently been shown that endocardium and myocardium interacted directly through tunneling nanotube–like structures extending from cardiomyocytes to endocardial cells, contributing to NOTCH1 activation [16]. Factors involved in the synthesis or degradation of cardiac jelly, a layer of extracellular matrix between endocardium and myocardium, also play essential roles in the process of chamber morphogenesis, including glycosaminoglycan proteins such as versican and ADAMTS family proteins [17,18]. The ANGPT1-TIE2 pathway plays a crucial role in cardiovascular development [19–22]. ANGPT1 is expressed by cardiomyocytes, particularly in atrial myocardium and ventricular trabeculae, and participates in the atrial morphogenesis by regulating the spatiotemporal degradation of cardiac jelly [19]. The endocardial specific deletion of *Tek* resulted in the fewer but thicker ventricular trabeculae as well as impaired endocardial sprouting, potentially via the paracrine suppression of retinoic acid signaling and proliferation in trabecular cardiomyocytes [23].

Endothelial TIE1 shares high homology with TIE2 and could form TIE1/TIE2 heterodimers [24]. TIE1 has been shown to participate in the regulation of blood vascular and lymphatic network formation and also aortic valve development [25–29]. It has recently shown that TIE1 and TIE2, via the PI3K-AKT-mediated signaling pathway for the protein stability of COUP-TFII, regulate venous specification [28,30]. Loss of the transcription factor COUP-TFII was reported to disrupt both the vein and atrial development [31–33]. *Tie1* mutations or variants have also been linked to lymphatic disorders [34,35]. It remains to be characterized whether Tie1 mutations could affect heart structure and function, and how TIE1 participates in the process of cardiac wall morphogenesis. To investigate the role of TIE1 and TIE2 in the process of endocardial cell-mediated chamber formation, we employed genetic mouse models targeting *Tie1*, *Tek* (encoding TIE2) or both at

different developmental stages. Based on the analysis of the published single cell RNA sequencing data (scRNA-seq) by Feng et al. [36] and the RNA-seq analysis of atria and ventricles from the *Tie1* mutant and littermate control mice, we found in this study that *Tie1* and *Tek* expression were higher in atrial than ventricular endocardial cells. TIE1 is differentially required for the atrial and ventricular trabeculation, acting in synergy with TIE2.

Materials and Methods

Mouse models

All animal procedures performed conform the guidelines from Directive 2010/63/EU of the European Parliament on the protection of animals used for scientific purposes; and the experiment protocols were approved by the Animal Care Committee of Soochow and Nanjing University Animal Center (MARC-AP#YH2/SUDA20250507A03). All the mice used in this study were housed in a SPF (specific pathogen free) animal facility with a 12/12 hours dark/light cycle and were free to food and water access. Normal mouse diet (Suzhou Shuangshi Experimental Animal Feed Technology, Co, Ltd) and cage bedding (Suzhou Baitai Laboratory Equipment, Co, Ltd) were used. Two genetically modified mouse models targeting *Tie1* gene were employed in this study. One mouse line targets TIE1 intracellular kinase domain (ICD), with exon 15 and exon 16 floxed, $Tie1ICD^{Flox/Flox}$[37]. The other line is a knockout first mouse model established from EUCOMM embryonic stem cells (EPD0735-3B07) targeting *Tie1* gene ($Tie1^{tm1a/tm1a}$), in which targeting cassette is recombined downstream of exon 7 (with exon 8 floxed) [28]. *Tek* knockout mouse model was generated as previously reported [38] and was crossbred with $Tie1^{\Delta ICD/\Delta ICD}$ mouse model to obtain *Tie1ICD* and *Tek* double knockout mice ($Tie1^{\Delta ICD/\Delta ICD};Tek^{+/-}$). To generate mice with endothelial cell–specific gene deletion mouse models, we employed the $Cdh5\text{-}Cre^{ERT2}$ mouse line [39]. In all the phenotype analysis, wildtype or heterozygous littermates were used as controls. For the genotyping of *Tie1* and *Tek* mouse lines, the primers used were as previously described [28,37]. The genetic background of $Tie1^{tm1a/tm1a}$ is on C57BL/6 N, and the other lines are on C57BL/6J or C57BL/6J/SV129. Mice were sacrificed by asphyxiation with rising concentration of carbon dioxide gas, followed by cervical dislocation and tissue collection.

Induced gene deletion

Induction of gene deletion was performed as previously described by the tamoxifen treatment [28,38,40]. Briefly, pregnant mice were treated with tamoxifen (Sigma-Aldrich, T5648-5G) at E10.5-E11.5, E12.5-14.5 or E12.5-15.5 (1 mg/per mouse for 2-4 consecutive days by intraperitoneal injection) and embryos were collected for analysis at the specified stages. For the postnatal studies, new-born pups were treated by four daily intragastric injections of tamoxifen starting from postnatal day 1 (P1, 60 μg/per mice daily). Tissues were collected for analysis at postnatal day 21. The genotypes of the *Tie1/Tek* knockout and control mice are as follows: $Tie1ICD^{Flox/-};Cdh5\text{-}Cre^{ERT2}$ named as $Tie1ICD^{iECKO}$, $Tek^{Flox/-};Cdh5\text{-}Cre^{ERT2}$ named as Tek^{iECKO}, $Tie1ICD^{Flox/-};Cdh5\text{-}Cre^{ERT2};Tek^{+/-}$ named as $Tie1ICD^{iECKO};Tek^{+/-}$.

Embryo preparation

To investigate the developmental process of cardiac chamber formation, female mice were mated in the late afternoon and vaginal plugs were checked in the morning of the following day. The embryonic stages are estimated considering midday of the day on which the vaginal plug is present as embryonic day 0.5 (E0.5). Tail tips from mutant and control embryos were used for genotyping, and heart tissues from the embryos were collected for the subsequent histology and RNA analysis. For the RNA preparation, heart tissues were harvested and placed in cold PBS. The residual blood from the hearts was cleaned and heart tissues were snap-frozen in liquid nitrogen. For the separate analysis of atria and ventricles, heart tissues were collected and dissected before snap-freezing.

Immunostaining

For the frozen tissue section staining, tissues were collected and fixed in 4% paraformaldehyde for 2 hours at 4°C, followed by the incubation in 20% sucrose overnight before being embedded in optimal cutting temperature (OCT) compound. Frozen sections (10 μm) were used for the immunostaining analysis of cardiac chamber structures and coronary vessels. For the visualization of atrial internal muscular network-trabeculae structures, the whole-mount immunostaining was performed. Heart tissues were fixed in 4% paraformaldehyde overnight at 4°C, followed by blocking with 3%(w/v) skim milk in PBS-TX (0.3% Triton X-100) and incubating with the primary antibodies. The antibodies used were: hamster anti-mouse PECAM1(MAB1398Z; Millipore); rat anti-mouse CD31 (553370; BD Pharmigen), rat anti-mouse Endomucin (14-5851; eBioscience), goat-anti-mouse DLL4 (AF1389; R&D) and goat anti-human TIE1 (AF619; R&D). Appropriate Alexa 488(Invitrogen), Cy3(Jackson ImmunoReaearch) conjugated secondary antibodies were used. All fluorescently labeled samples were mounted and analyzed with a confocal microscope (Olympus Flueview 3000) or Leica MZ16F fluorescent dissection microscope. For comparison, the parameters were kept consistent for all the confocal microscopic imaging in this study.

Bulk RNA sequencing analysis of atria and ventricles

For the bulk RNA-seq analysis of heart tissue, the whole hearts from mutant and control embryos were collected. Atria and ventricles were separated and tissues from two embryos with the same genotype (*Tie1*$^{tm1a/tm1a}$ and *control*) were pooled for the RNA preparation and further analysis. According to the manufacturer's instructions, total RNA was extracted from the tissues using Trizol (Invitrogen). The procedures for the RNA-seq analysis were performed as previously reported [28]. Briefly, sequencing was performed on DNBSEQ platform with PE150 (read length, BGI-Shenzhen, China), and the sequencing data were processed according to the predefined analysis pipeline. The differential expression analysis was conducted using the R package DESeq2 (v 1.42.1). Functional enrichment analysis was performed using clusterProfiler (v4.10.1) and org.Mm.eg.db (v 3.18.0). The hallmark gene sets used in the GSEA (Gene Set Enrichment Analysis), including the hallmarks for trabeculation and EC migration, are mainly defined according to the transcriptome atlas of murine endothelial cells, the molecular signatures database (mh.all.v2024.1.Mm.symbols) and the related GO terms [28,41,42]. The raw and processed data of RNA-seq analysis will be deposited in GEO after the publication.

Single cell RNA-seq data analysis

The single-cell RNA sequencing data by Feng et al. [36] were processed and analyzed with the Seurat package (v5.2.1) following the same parameters and criteria as described to ensure consistency and comparability. Major cell types were annotated based on established marker genes: pan-cardiomyocyte (*Ttn*), atrial cardiomyocytes (*Sln*), ventricular cardiomyocyte (*Myl2*), pan-endothelial cells (*Pecam1*), endocardial cells (*Npr3*), coronary endothelial cells (*Fabp4*), epicardial cells (*Wt1*, *Tbx18*, and *Aldh1a2*), fibroblast-like cells (*Postn*), mural cells (*Pdgfrb*), red blood cells (*Hba-a1*), macrophages (*Adgre1*). Following the identification of endocardial cells, subsequent analysis was performed using the Seurat package and normalized by the "LogNormalize" method, highly variable genes were identified with the 'FindVariableFeatures" function (selection.method = "vst", nfeatures = 2000). The optimal number of principal components (dims = 1:22) was determined by the ElbowPlot method. Cells were then clustered using the "FindNeighbors" and "FindClusters" functions (dims= 1:16, resolution = 0.5). Finally, Unsupervised clustering of cells will be performed by "RunUMAP" and gene expression was visualized with "FeaturePlot". Ligand–receptor interactions between cardiomyocytes and endocardial cells during the embryonic stage (E10.5-E18.5) were identified using the CellChat package (v1.6.1). Atrial and ventricular cell subsets were analyzed separately using the mouse ligand-receptor database (CellChatDB.mouse) and communication probabilities were computed (min.cells = 10) to identify significant interactions.

Quantitative analysis of cardiac wall and trabeculae

For the quantification of trabecular structures in atria and ventricles, the EMCN positive areas was measured. The PECAM1 positive area was quantified to indicate the coronary vessels within the ventricular wall. The cardiac wall thickness was also measured as described in the supplemental figure 2. For the quantitative analysis of dorsal coronary veins, images were taken under a fluorescence microscope and kept constant near the venous sinus for all of the samples. Horizontal lines were evenly laid on the images, and the diameters of veins crossed with these lines were measured and analyzed using Image Pro Plus (Media Cybernetics, Inc., Bethesda, MD). The ratio of heart to embryo length was used to represent heart size. The starting point for the heart measurement was the junction of aorta and pulmonary artery, and the junction of left and right ventricles at the apex as the end point. All the quantification was measured and analyzed by using Image Pro Plus. Furthermore, we also performed the measurement of cardiac trabecular complexity by the Fractal analysis. Fractal dimensions were derived from confocal images of hearts from *Tie1* mutants and control mice. Quantification was carried out using ImageJ with the Fraclac plugin (including 6 grid orientations).

Statistical analysis

Data analyses were performed using GraphPad Prism (version 8.0). For the 2-group comparison, the unpaired t test was performed with Welch correction if data passed the D'Agostino-Pearson normality test, or the unpaired nonparametric Mann-Whitney U test was applied. Data are expressed as mean ± SD. All statistical tests were 2-sided.

Results

Higher TIE1 and TIE2 in atrial than ventricular endocardial cells

To dissect the transcriptional dynamics of key endothelial regulators during the murine heart development, we analyzed the published single-cell transcriptomic dataset spanning the murine embryonic development (E10.5-E18.5) [36]. We found that *Tie1*, and *Tek* were highly expressed in endocardial cells (*Pecam1*$^{+}$, *Npr3*$^{+}$) while the coronary EC gene such as the coronary endothelial marker *Fabp4* was lowly expressed in endocardial cells (Fig. 1A-B, Supplemental Fig. 1A-C). Interestingly, we found that the transcript levels of *Tie1*, and *Tek* were higher in the atrial endocardial cells than those of ventricles, especially at embryonic stages up to E14.5 when the structures of four-chambered hearts were established (Table 1). In contrast, it appears that the *Angpt1* transcript level was higher in atrial than ventricular cardiomyocytes (Fig. 1A-B, Table 1).

To investigate mechanisms underlying the murine atrial trabeculation, we first analyzed the dynamic processes of cardiac chamber morphogenesis by the immunostaining analysis of endomucin (EMCN) for trabeculae and PECAM1 for coronary vessels (embryonic day 10.5-E18.5). The quantification methods for atrial and ventricular trabecular areas, wall thickness and vessel density were shown in Supplemental Fig. 2A. As shown in Supplemental Fig. 2B, the heart tube became looped to form the preliminary chamber structures at E10.5, including the initiation of interventricular septum. While there appeared to have some wavy edges or the budding of endocardium in atria (E10.5), trabecular structures were readily detectable in ventricles at this stage. Therefore, atrial wall morphogenesis occurs later than that of ventricles, which initiates the trabeculation process around E8.5 when endocardial cells migrate through cardiac jelly to form anchor points with compact myocardium [15]. We found that pectinate muscles, defined as the atrial trabeculae, became detectable in the atria at E12.5 (Supplemental Fig. 2B). The formation of interventricular septum was completed by E14.5, establishing the four-chambered heart. By E16.5 or later stages (Supplemental Fig. 2C), the atrial and ventricular trabeculae gradually formed a complex network. As shown in Supplemental Fig. 2D-G (Supplemental Table 1), the trabecular areas in both the atria and ventricles gradually increased, being greater in the right atria (RA) than that in the left atria (LA, Supplemental Fig. 2D). There was no obvious difference in the trabecular areas between the left and right ventricles (Supplemental Fig. 2E). The ventricular

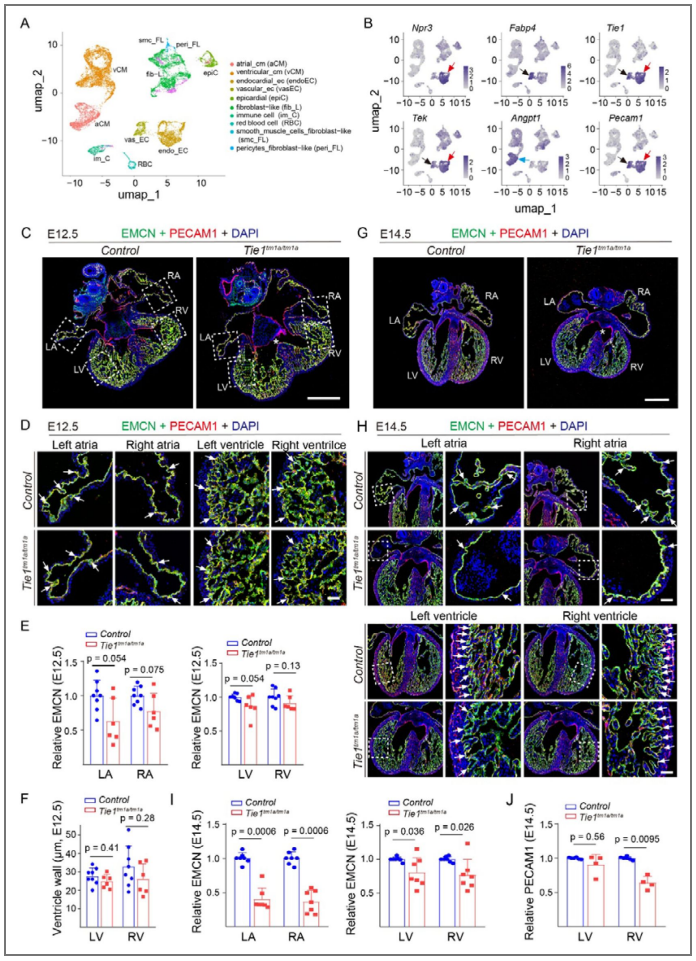

Fig. 1. Analysis of TIE1 expression in endocardial cells by the single cell RNA-seq data and its role in cardiac trabeculation during embryogenesis.

A-B. Analysis of the single-cell RNA-seq data of embryonic hearts from E10.5 to E18.5 by Feng et al. Nat Commun 2022 (DOI: 10.1038/s41467-022-35691-7). UMAP visualization of 10 distinct cell clusters in the murine hearts during embryogenesis (E10.5 to E18.5, A). *Tie1* and *Tek* are highly expressed in the endocardial cell population (*Npr3*$^{+}$) as shown in feature plots. *Angpt1* are highly expressed in the atrial cardiomyocytes (B). Black arrows point to the coronary EC population (*Fabp4*$^{+}$). Red arrows point to the endocardial cell population (*Npr3*$^{+}$). Blue arrows point to the atrial cardiomyocytes. The quantitative results are shown in Table 1. C-J. Analysis of heart trabeculae of *Tie1*$^{tm1a/tm1a}$ and littermate controls by immunostaining for EMCN (endomucin; green), PECAM1 (platelet endothelial cell adhesion molecule 1; red) and DAPI (blue) at E12.5 (C-D) and E14.5 (G-H). Note that *Tie1*$^{tm1a/tm1a}$ mice displayed defective trabeculation in the atrium (white arrows) and sparse trabecular structures in the ventricles (white arrows) at E12.5, with more severe defects by E14.5, lacking atrial trabeculae (white arrows) and sparser ventricular trabeculae (white arrows). Asterisks in C and G point to the delayed formation of interventricular septum in *Tie1*$^{tm1a/tm1a}$ mice. Arrows point to the trabecula-associated endocardium. E-F. Quantification of the EMCN-positive area in the atrial and ventricular trabeculae at E12.5 (E, LA: *Tie1*$^{tm1a/tm1a}$: 0.63±0.33, n=6; *Control*: 1.00±0.22, n=8; *P*=0.054. RA: *Tie1*$^{tm1a/tm1a}$: 0.77±0.26, n=6; *Control*: 1.00±0.13, n=8; *P*=0.075. LV: *Tie1*$^{tm1a/tm1a}$: 0.86±0.16, n=6; *Control*: 1.00±0.046, n=8; *P*=0.054. RV: *Tie1*$^{tm1a/tm1a}$: 0.91±0.11, n=6; *Control*: 1.00±0.12, n=8; *P*=0.13.). Quantification of the ventricular wall thickness (F, LV: *Tie1*$^{tm1a/tm1a}$: 24.87±3.70 μm, n=6; *Control*: 27.67±4.52 μm, n=8; *P*=0.41. RV: *Tie1*$^{tm1a/tm1a}$: 26.01±8.42 μm, n=6; *Control*: 32.84±11.21 μm, n=8; *P*=0.28.). I-J. Quantification of the EMCN-positive area in the atrial and ventricular trabeculae at E14.5 (I, LA: *Tie1*$^{tm1a/tm1a}$: 0.40±0.16, n=7; *Control*: 1.00±0.079, n=7; *P*=0.00060. RA: *Tie1*$^{tm1a/tm1a}$: 0.36±0.17, n=7; *Control*: 1.00±0.092, n=7; *P*=0.00060. LV: *Tie1*$^{tm1a/tm1a}$: 0.81±0.22, n=7; *Control*: 1.00±0.033, n=7; *P*=0.036. RV: *Tie1*$^{tm1a/tm1a}$: 0.77±0.23, n=7; *Control*: 1.00±0.040, n=7; *P*=0.026.). Quantification of the PECAM1-positive area in ventricular walls (J, LV: *Tie1*$^{tm1a/tm1a}$: 0.91±0.15, n=4; *Control*: 1.00±0.013, n=6; *P*=0.56. RV: *Tie1*$^{tm1a/tm1a}$: 0.64±0.096, n=4; *Control*: 1.00±0.024, n=6; *P*=0.0095.). The quantification data of mutant mice was normalized against that of littermate control mice. In E-J, statistical analysis was performed using the unpaired nonparametric Mann-Whitney U test. Values are represented as means ± SD of at least three independent technical replicates. LA, Left atria, RA, Right atria, LV, Left ventricle, RV, Right ventricle, Scale bar: Scale bar: 400 μm in C and G, 50 μm in D and H.

	Tie1		*Tek*		*Angpt1*	
	Atria (mean±sd)	Ventricle (mean±sd)	Atria (mean±sd)	Ventricle (mean±sd)	Atria (mean±sd)	Ventricle (mean±sd)
E10.5	1.34±0.50 (n = 9)	1.17±0.39 (n = 16)	1.37±0.54 (n = 10)	1.31±0.50 (n = 17)	0.53±0.49 (n = 50)	0.28±0.41 (n = 197)
E12.5	1.54±0.43 (n = 5)	1.27±0.47 (n = 220)	1.26±0.50 (n = 4)	1.17±0.48 (n = 215)	0.95±1.19 (n = 6)	0.29±0.40 (n = 665)
E14.5	1.60±0.49 (n = 9)	1.41±0.48 (n = 72)	1.43±0.39 (n = 8)	1.37±0.48 (n = 61)	1.13±0.45 (n = 47)	0.18±0.34 (n = 322)
E16.5	1.41±0.47 (n = 89)	1.35±0.49 (n = 35)	1.18±0.45 (n = 84)	1.49±0.45 (n = 33)	1.41±0.55 (n = 404)	0.17±0.41 (n = 112)
E18.5	1.26±0.40 (n = 137)	1.35±0.47 (n = 30)	1.15±0.45 (n = 136)	1.24±0.43 (n = 25)	1.15±0.67 (n = 455)	0.098±0.28 (n = 277)

Table 1. The transcript levels of *Tie1*, *Tek* in atrial and ventricular endocardial cells and *Angpt1* in atrial and ventricular cardiomyocytes during the embryonic stage from E10.5-E18.5 (based on the published scRNA-seq data, Feng et al., Nat Commun 2022; DOI: 10.1038/s41467-022-35691-7).

Values are represented as means ± SD and the number referred to cell counts.

wall thickness increased rapidly after E12.5, with the left ventricular wall being thicker than that of the right ventricular wall by E18.5 (Supplemental Fig. 2F), accompanied by the increase of coronary vessel density (Supplemental Fig. 2G).

Differential requirement of TIE1 in atrial and ventricular trabeculation

To study the role and mechanism underlying TIE1 function in cardiac chamber morphogenesis, we employed two genetically modified mouse models targeting *Tie1*, including $Tie1^{tm1a/tm1a}$ and $Tie1^{\Delta ICD/\Delta ICD}$. The effects of *Tie1* gene deletion on atrial and ventricular trabeculae were analyzed at different developmental stages (including E12.5, E14.5 and E17.5). TIE1 deficiency led to an impaired trabeculation in the atria, characterized by a decrease of trabecular structures at E12.5, while the formation of ventricular trabeculae was not obviously affected at the same stage (Fig. 1C-D). Shown in Fig. 1E was the quantification of trabecular areas in atria and ventricles. The thickness of left and right ventricular walls at this stage was shown in Fig. 1F. Consistently, the atrial trabeculae were almost absent in the *Tie1* mutant mice at E14.5, while trabeculae became sparse in both left and right ventricles (Fig. 1G-I). There was also a trend of decrease in the coronary vessel density upon TIE1 deficiency (Fig. 1J). By the later stages of embryonic development (E17.5), TIE1 deficiency resulted in more severe cardiac defects, including a significant reduction in heart size, absence of atrial trabeculae, and disorganized trabecular structures in ventricles, together with a decrease in the ventricular wall thickness as well as the coronary vessel density (Fig. 2A-F). The defective atrial trabecula formation was also validated in another *Tie1* mutant line targeting its intracellular kinase domain ($Tie1^{\Delta ICD/\Delta ICD}$, Supplemental Fig. 3A-E). Consistent with the above results, TIE1 deficiency resulted in the lack of atrial trabeculation while trabeculae in ventricles became sparse in *Tie1* mutants at E14.5. There was also a trend of decrease in ventricular wall thickness as well as the coronary vessel density in the $Tie1^{\Delta ICD/\Delta ICD}$ mice. Consistently, the atrial trabecular defects could also be reflected by the fractal analysis of cardiac trabecular complexity in atria from *Tie1* mutant and control mice at E14.5 and E17.5 using the Fraclac Plugin in ImageJ, while the relatively minor defects in the ventricles were not detected by the method ($Tie1^{tm1a/tm1a}$, Supplemental Fig. 4; Supplemental Table 2). Consistent with the previous observation [28], the lack of TIE1 also disrupted the coronary vein formation at the later embryonic stages (E14.5 and E17.5), including the decrease of vein diameter and the increase of vein-associated angiogenic sprouting (Supplemental Fig. 5A-D).

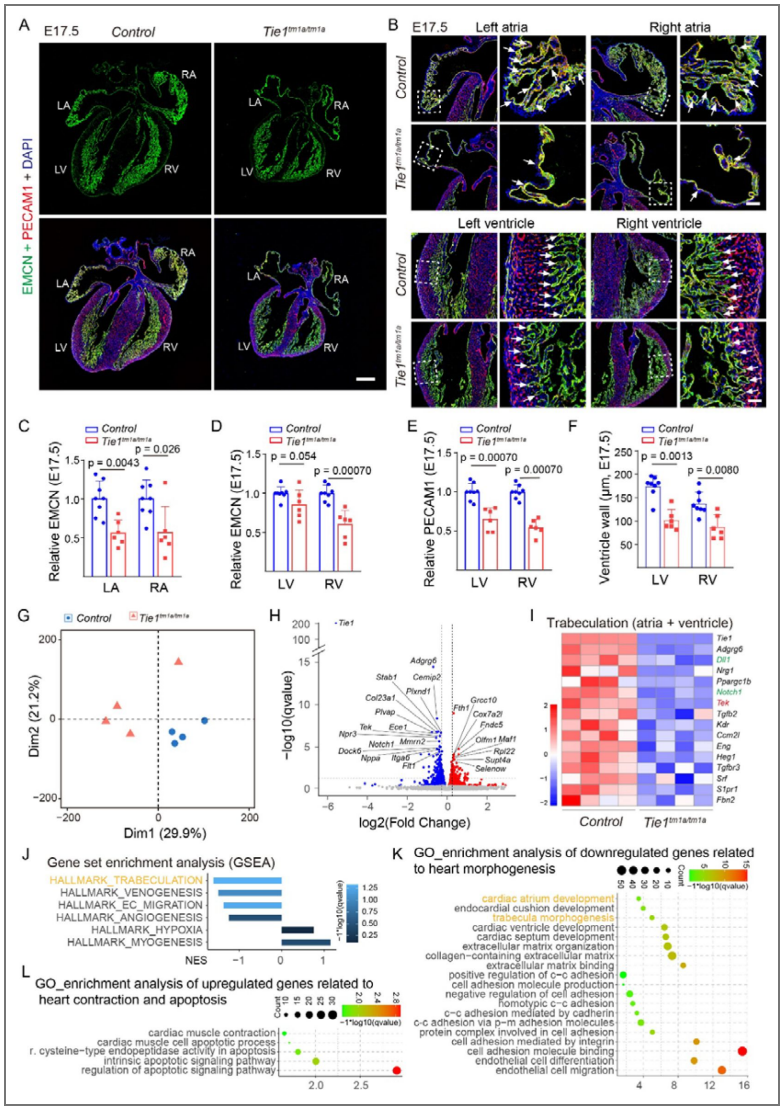

Fig. 2. Suppression of cardiac trabeculation-related gene expression by the loss of TIE1.

A-B. Analysis of heart trabeculae of *Tie1*$^{tm1a/tm1a}$ and littermate controls by immunostaining for EMCN (green), PECAM1 (red) and DAPI (blue) at E17.5. Note that the ventricular trabeculae of *Tie1*$^{tm1a/tm1a}$ mice become sparse compared with those of control mice (white arrows). Arrows point to the trabecula-associated endocardium. **C-F**. Quantification of the EMCN-positive area in the atrial and ventricular trabeculae (**C**, LA: *Tie1*$^{tm1a/tm1a}$: 0.56±0.16, n=6; *Control*: 1.00±0.22, n=8; *P*=0.0043. RA: *Tie1*$^{tm1a/tm1a}$: 0.57±0.33, n=6; *Control*: 1.00±0.24, n=8; *P*=0.026. **D**, LV: *Tie1*$^{tm1a/tm1a}$: 0.86±0.18, n=6; *Control*: 1.00±0.082, n=8; *P*=0.054. RV: *Tie1*$^{tm1a/tm1a}$: 0.61±0.18, n=6; *Control*: 1.00±0.10, n=8; *P*=0.00070). Quantification of the PECAM1-positive area in ventricular walls (**E**, LV: *Tie1*$^{tm1a/tm1a}$: 0.66±0.14, n=6; *Control*: 1.00±0.11, n=8; *P*=0.00070. RV: *Tie1*$^{tm1a/tm1a}$: 0.55±0.10, n=6; *Control*: 1.00±0.088, n=8; *P*=0.00070.). Quantification of the ventricular wall thickness (**F**, LV: *Tie1*$^{tm1a/tm1a}$: 101.97 ± 22.44 μm, n=6; *Control*: 174.09 ± 22.84 μm, n=8; *P*=0.0013. RV: *Tie1*$^{tm1a/tm1a}$: 87.14±26.20 μm, n=6; *Control*: 137.35±24.06 μm, n=8; *P*=0.0080.) at E17.5. Except the ventricular wall thickness, the quantification data of mutant mice was normalized against that of littermate control mice. **G-L**. RNA-seq analysis of whole hearts of *Tie1*$^{tm1a/tm1a}$ and littermate controls (E14.5, n=4 per group). **G**. PCA analysis showed that *Tie1*$^{tm1a/tm1a}$ and *control* groups were divided into two clusters. **H**. Volcano plot visualization of the differentially expressed genes (DEGs, P-value ≤ 0.05, |Log2Foldchange| > 0). **I**. Heatmap of significantly downregulated cardiac trabeculation genes (P-value ≤ 0.05). **J**. GSEA analysis showed the decrease of enrichment in trabeculation, venous development, and endothelial cell migration pathways. **K-L**. GO analysis revealed that gene related to cardiac chamber morphogenesis and trabeculae development, extracellular matrix, cell adhesion and endothelial migration/differentiation were significantly downregulated (**K**), while cardiac contraction and apoptosis related genes were significantly upregulated (**L**). In C-F, statistical analysis was performed using the unpaired nonparametric Mann-Whitney U test. Values are represented as means ± SD of at least three independent technical replicates. LA: Left atria, RA: Right atria, LV: Left ventricle, RV: Right ventricle; Scale bar: 400 μm in A, 50 μm in B; c-c: cell-cell, p-m: plasma membrane in K.

Alteration of atrial versus ventricular gene regulatory network upon TIE1 deficiency

To explore the mechanism underlying TIE1 in heart development, we performed the RNA sequencing (RNA-seq) analysis of hearts to examine the alteration of cardiac transcriptome upon TIE1 deficiency. Lack of TIE1 led to a dramatic change in the overall transcriptional profile (Fig. 2G-L), including the suppression of gene expression related to the endocardial / endothelial development and cardiac chamber morphogenesis, such as *Tek* (normalized by *Pecam1*, $Tie1^{tm1a/tm1a}$: 0.89 ± 0.031, n=4; *WT*: 1.00 ± 0.12, n=4; $P = 0.057$.). Specifically, pathways related to extracellular matrix, cell adhesion and endothelial cell migration were downregulated (Fig. 2K), while the cardiac contraction and cell apoptosis pathways were upregulated (Fig. 2L). This was further confirmed by the GSEA analysis using the custom gene sets (Fig. 2J). The gene sets included the following entries based on the GO database (HALLMARK_TRABECULATION, HALLMARK_EC_MIGRATION) and the fifty-three entries from the previous publication [28]. Consistent with previous reports [28], TIE1 deficiency led to the downregulation of venous genes. In addition, key regulatory factors for cardiac trabecular development were downregulated, including *Adgrg6* (adhesion G protein-coupled receptor G6), *Nrg1* (neuregulin 1), and *Notch1* (Notch receptor 1) and *Dll1* (Delta Like Canonical Notch Ligand 1). Notably, we found that the expression of the TIE receptor family member *Tek* was also significantly reduced (Fig. 2I), suggesting that TIE1 acts, at least partially, via TIE2 in the regulation of cardiac trabecular morphogenesis.

To better visualize the trabecular structures, particularly the atrial internal muscular network, we performed the wholemount immunostaining of the hearts at the four-chambered stage. As shown in Fig. 3A, TIE1 deficiency led to the absence of the atrial trabecular network, with minor defects in the ventricles including a trend of sparse trabeculae (the 3D views shown in Supplemental Fig. 6). To further investigate the differential requirement of TIE1 in atrial and ventricular trabeculation, we collected atria and ventricle tissues separately from *Tie1* mutant and control mice (E14.5) for the RNA-seq analysis. We found that the number of differentially expressed genes was greater in atria than in the ventricles after the loss of TIE1 (Fig. 3B-G). Similar to the results from the whole heart RNA-seq analysis, the transcript levels of genes related to atrial development was decreased. Although a similar trend of decrease in genes involved in the cardiac morphogenesis were also observed in the ventricles, the enrichment levels and the number of genes involved were much lower in ventricles than in atria. Specifically, 17 trabecula-related genes were downregulated in the atria, while there was only 8 in the ventricles. Notably, *Tek* and *Dll1* were downregulated in both the atria and ventricles while *Notch1* only in atria of *Tie1* mutant mice (Fig. 3F-G; Supplemental Fig. 3F-G; Supplemental Table 3 and Supplemental Table 4). Interestingly, the expression of endothelial *Tie1*, *Tek* and *Notch1* was higher in atria than in ventricles (Fig. 3H, Supplemental Fig. 1D, Supplemental Table 5). The top GO terms enriched for the up- or down-regulated genes were related to the biological processes of heart development, including those in trabecular formation, extracellular matrix organization and binding, intercellular adhesion and endothelial cell migration in both atria and ventricles (Fig. 3I-J). In addition, the analysis of scRNA-seq data for the ligand-receptor interactions showed that the atrial_EC (endocardial cells) and atrial_CM (cardiomyocytes) exhibited stronger ANGPT1-TIE2 signaling compared with those in ventricles (Supplementary Fig. 1E). This may account for the differential requirement of TIE1 and also TIE2 in the process of atrial versus ventricular trabeculation.

Stronger ANGPT1-TIE2 interactions among atrial endocardium and myocardium

Using the published scRNA-seq data [36], we also analyzed the ligand-receptor interactions among endocardial cells and cardiomyocytes in atria and ventricles respectively during the embryonic stage (E10.5-E18.5). We found that the ANGPT1-TIE2 signaling between atrial cardiomyocytes and endocardial cells was stronger than that in ventricles (Supplemental Fig. 1E). Consistently, the

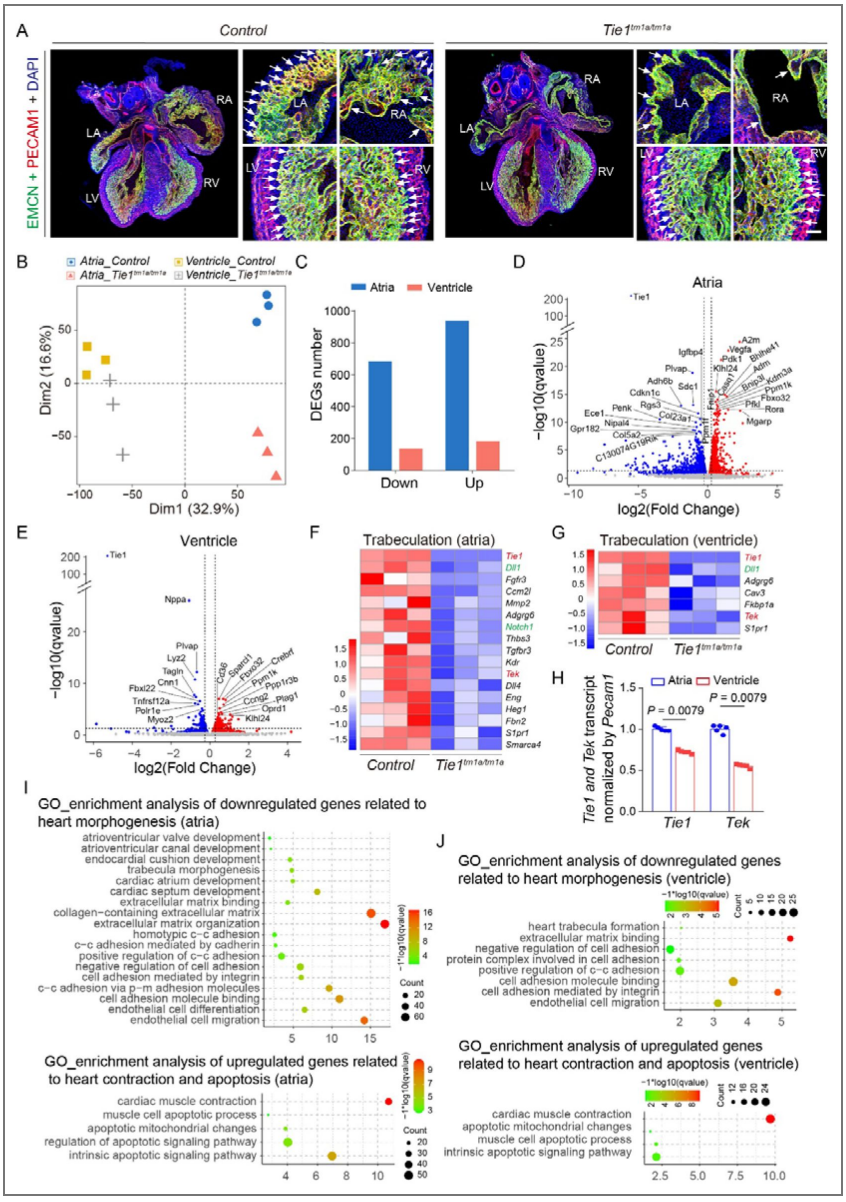

Fig. 3. Differential effect of *Tie1* deficiency on atrial versus ventricular trabeculation related gene network.

A. Visualization of heart trabeculae structure of *Tie1*$^{tm1a/tm1a}$ and littermate controls by whole-mount immunostaining for EMCN (green), PECAM1 (red) and DAPI (blue) at E14.5. Note that *Tie1* deletion resulted in the loss of atrial trabecular network with minor defects with ventricular trabecular structures (white arrows). Arrows point to the trabecula-associated endocardium. **B-J**. RNA-seq analysis of atrium and ventricles of *Tie1*$^{tm1a/tm1a}$ and littermate controls (E14.5, n=3 per group). **B**. PCA analysis results showed clear separation between the atria and ventricles of *Tie1*$^{tm1a/tm1a}$ and control mice. **C**. Differential expression analysis (P-value ≤ 0.05, |log2(Foldchange)| ≥ 0.15) identified over 693 down-regulated and 948 up-regulated atrial genes, while 144 down-regulated and 190 up-regulated genes in ventricles. **D-E**. Volcano plots of atrial (**D**) and ventricular (**E**) differential expressed genes (DEGs). **F-G**. Heatmap showed significantly downregulated (P-value ≤ 0.05) heart trabeculation genes in atrium (**F**) and ventricles (**G**), including *Tek*, *Dll1* and *Notch1*. **H**. Quantitation of *Tie1* and *Tek* transcript levels (normalized by *Pecam1*) in atrium and ventricles of *Tie1*$^{tm1a/tm1a}$ and littermate controls (*Tie1*: Ventricles: 0.72 ± 0.021, n = 5; Atria: 1.00 ± 0.026; *P* = 0.0079. *Tek*: Ventricle: 0.55 ± 0.024; Atria: 1.00 ± 0.048; *P* = 0.0079). **I-J**. GO enrichment analysis of the DEGs in atrium and ventricles including the heart trabecula morphogenesis, extracellular matrix, cell adhesion and endothelial migration related process down-regulated while genes related to the cardiac contraction, apoptosis process up-regulated. There was a more obvious enrichment detected in the atria. In H, statistical analysis was performed using the unpaired nonparametric Mann-Whitney U test. Values are represented as means ± SD of at least three technical replicates. LA: left atria, RA: right atria, LV: left ventricle, RV: right ventricle; Scale bar: 50 μm in A; c-c: cell-cell, p-m: plasma membrane in I-J.

crucial role of endothelial TIE2 in the atrial trabeculation was validated in this study by employing a conditional knockout mouse model targeting *Tek* (also known as *Tie2* gene; $Tek^{Flox/-}$; $Cdh5\text{-}Cre^{ERT2}$; named Tek^{iECKO}). As the complete knockout of *Tek* gene leads to embryonic lethality before E10.5, we first performed the induced endothelial *Tek* deletion starting from E12.5 (Fig. 4A-B). We found that TIE2 insufficiency led to an obvious decrease of trabeculae in the atrium 48 h later (E14.5), while there were no obvious defects observed in the ventricular trabeculae at this stage (Fig. 4C-E). The coronary vessel density in the ventricular wall as well as the wall thickness, including left and right ventricles, were not obviously altered when examined 48 h later (Fig. 4F). In separate experiments with the induced gene deletion from E12.5 to E14.5, embryos were collected for the analysis at 72 hours (E15.5) or later (E17.5). The formation of atrial trabeculae was completely missing as shown in Fig. 4A, G-H. The defective trabecula formation was also detected in the ventricles, especially at later embryonic stages (E17.5, Fig. 4A, G-H). TIE2 insufficiency also led to the defective formation of the coronary veins as previously shown in skin and mesentery [30] (Supplemental Fig. 5E, G).

Synergy of TIE1 and TIE2 in atrial trabeculation

To investigate the synergistic effects of TIE1 and TIE2 in the regulation of cardiac morphogenesis, we generated a doubly knockout model targeting *Tie1* and *Tek* ($Tie1^{\Delta ICD/\Delta ICD}$; $Tek^{+/-}$). There were no obvious defects observed with the atrial or ventricular structures upon *Tie1* deficiency alone at E10.5 (Fig. 5A-B). Intriguingly, loss of *Tie1* combined with the heterozygous deletion of *Tek* suppressed both atria and ventricle development (E10.5), including reduced heart size, abnormal atrial chamber formation, and fewer trabecular structures in the ventricles (Fig. 5C-D), leading to embryonic lethality before E12.5.

To further explore the synergy of TIE1/TIE2 in the heart development at later stages of embryonic development, we generated an inducible mouse model with the endothelial deletion of *Tie1* combined with *Tek* heterozygous knockout ($Tie1ICD^{Flox/-}$;$Cdh5\text{-}Cre^{ERT2}$;$Tek^{+/-}$, named $Tie1ICD^{iECKO}$;$Tek^{+/-}$). The induced gene deletion was performed by the tamoxifen treatment starting from E10.5, and mice were sacrificed for analysis after 96 hours (E14.5). The gene deletion efficiency was confirmed by the immunostaining for PECAM1 plus TIE1. TIE1 insufficiency combined with the heterozygous loss of TIE2 led to the suppression of atrial trabeculation, while the trabeculae at both right and left ventricle became sparse and irregular (Fig. 5E-H). Furthermore, when the induced gene deletion was performed at E12.5, the defective atrial trabeculation were already detectable in the mutant mice 48 hours later (E14.5 $Tie1ICD^{iECKO}$;$Tek^{+/-}$; Fig. 6 A-D). Consistent with the observation with the endothelial *Tek* deletion for 48 hours, there was no obvious defects with the ventricular trabeculation, coronary vessel density and ventricular wall thickness ($Tie1ICD^{iECKO}$;$Tek^{+/-}$; Fig. 6D-E, Table 2). The disruption of cardiac trabeculation became more obvious when analyzed 72-96 hours later, particularly in atria but less severe with ventricles ($Tie1ICD^{iECKO}$; $Tek^{+/-}$, E15.5-E16.5; Fig. 6 F-G, Table 3). There was also a trend of decrease in coronary vessel density and ventricular wall thickness as shown at later stages (E16.5, Fig. 6 F, H, Table 3). In addition, the TIE1/TIE2 insufficiency also resulted in the disruption of cardiac vein development as shown in (Supplemental Fig. 5F, H), as previously reported in skin and retina [28].

Requirement of TIE receptors for the postnatal atrial trabecular remodeling

The role of TIE1 and its synergy with TIE2 in cardiac trabecular development was further confirmed at the neonatal stage ($Tie1ICD^{iECKO}$ or $Tie1ICD^{iECKO}$; $Tek^{+/-}$) with the induced gene deletion from postnatal day 1 (P1-4) and the analysis performed at P21. The *Tie1* deletion was confirmed by the vascular defects in retinas of $Tie1ICD^{iECKO}$ or $Tie1ICD^{iECKO}$; $Tek^{+/-}$mice as previously reported (Fig. 7B, E) [28]. TIE1 insufficiency alone had no obvious impact on the heart weight and also the atrial or ventricular trabeculation analyzed within three weeks (Fig. 7 A-D). Consistent with the studies at embryonic stages, the induced postnatal gene deletion ($Tie1ICD^{iECKO}$;$Tek^{+/-}$) showed the retarded heart development by the quantification of heart-body

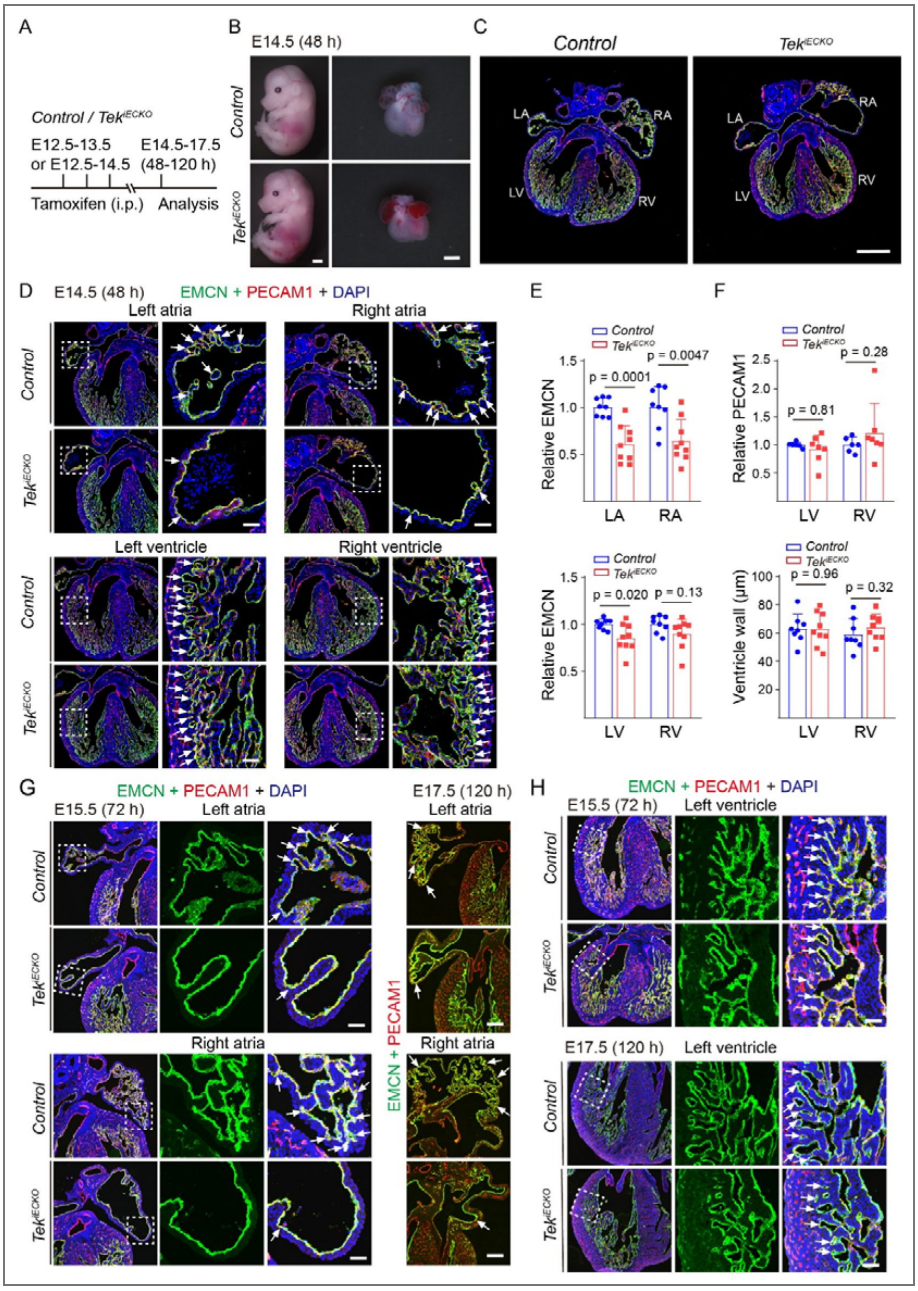

Fig. 4. Impaired atrial trabecular formation after TIE2 insufficiency.

A. Tamoxifen intraperitoneal (i.p.) administration and analysis scheme. **B-D**. Analysis of heart trabeculae of *Tek*^{iECKO} and littermate controls by immunostaining for EMCN (green), PECAM1 (red) and DAPI (blue) 48 hours later (tamoxifen treatment starting at E12.5). **E-F**. Quantification of the EMCN-positive area in the atrial and ventricular trabeculae (**E**, LA: *Tek*^{iECKO}: 0.60±0.20, n=9; *Control*: 1.00±0.097, n=8; *P*=0.00010. RA: *Tek*^{iECKO}: 0.64±0.23, n=9; *Control*: 1.00±0.22, n=8; *P*=0.0047. LV: *Tek*^{iECKO}: 0.85±0.15, n=9; *Control*: 1.00±0.057, n=8; *P*=0.020. RV: *Tek*^{iECKO}: 0.90±0.16, n=9; *Control*: 1.00±0.089, n=8; *P*=0.13.), quantification of the PECAM1-positive area in ventricular walls (**F**, LV: *Tek*^{iECKO}: 0.92±0.25, n=7; *Control*: 1.00±0.048, n=6; *P*=0.81. RV: *Tek*^{iECKO}: 1.22±0.53, n=7; *Control*: 1.00±0.13, n=6; *P*=0.28.) and quantification of the ventricular wall thickness (**F**, LV: *Tek*^{iECKO}: 62.35±11.70 μm, n=9; *Control*: 62.59±10.26 μm, n=8; *P*=0.96. RV: *Tek*^{iECKO}: 63.87± 9.19 μm, n=9; *Control*: 58.87±11.02 μm, n=8; *P*=0.32.) at E14.5. Except the ventricular wall thickness, the quantification data of mutant mice was normalized against that of littermate control mice. **G-H**. Analysis of heart trabeculae of *Tek*^{iECKO} and littermate controls by immunostaining for EMCN (green), PECAM1 (red) and DAPI (blue) 72 hours after the induced gene deletion or later (tamoxifen treatment starting at E12.5). Arrows point to the trabecula-associated endocardium. In E-F, statistical analysis was performed using the unpaired t test. Values are represented as means ± SD of at least three independent technical replicates. LA: left atria, RA: right atria, LV: left ventricle, RV: right ventricle; Scale bar: 500 μm (embryo) and 400 μm (heart) in B, 400 μm in C, 50 μm in D, G, H.

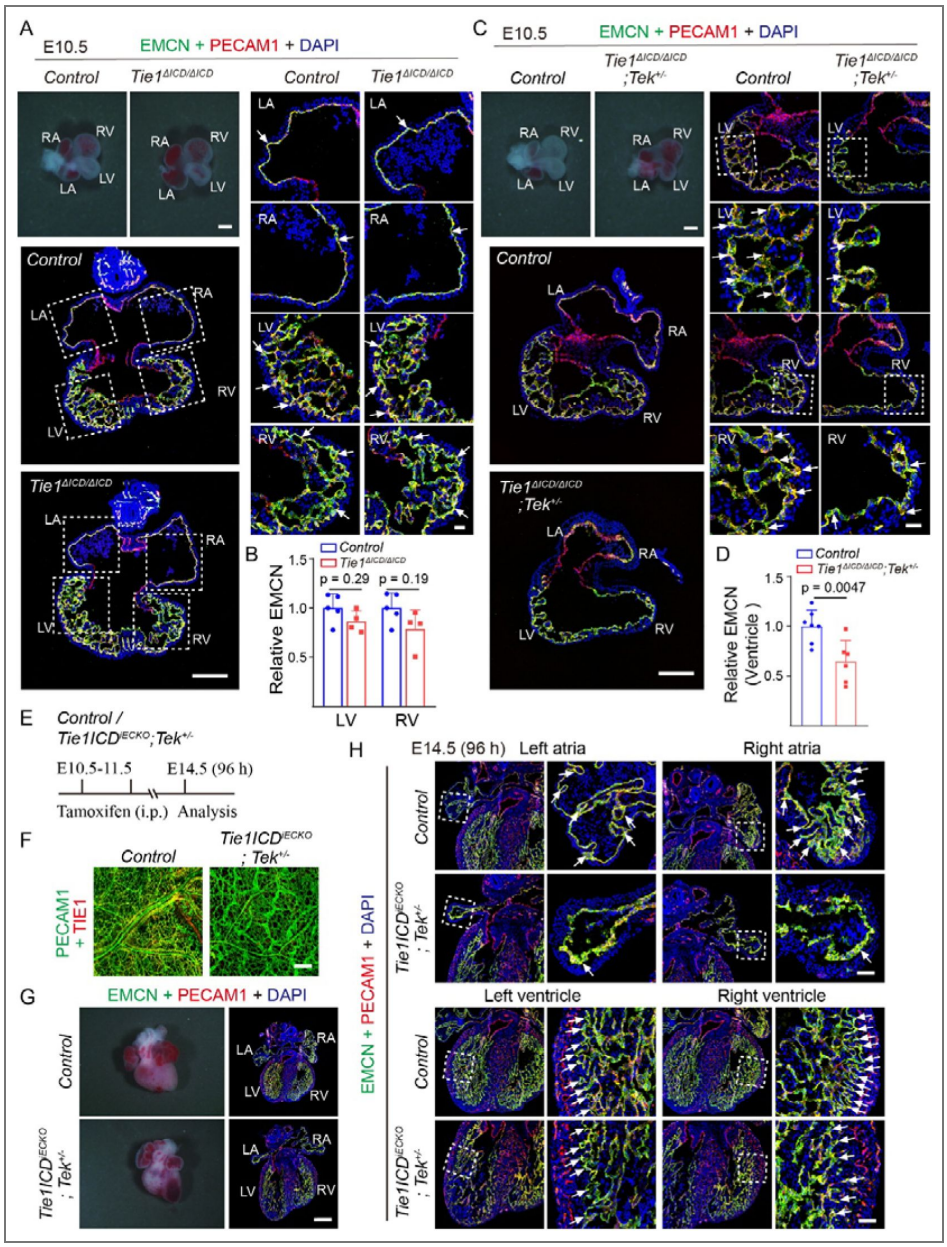

Fig. 5. Developmental requirement of TIE1 and TIE2 in atrial and ventricular chamber morphogenesis.

A-D. Analysis of heart trabeculae of *Tie1*$^{\Delta ICD/\Delta ICD}$, *Tie1*$^{\Delta ICD/\Delta ICD}$*;Tek*$^{+/-}$ and littermate controls by immunostaining for EMCN (green), PECAM1 (red) and DAPI (blue) at E10.5. Note that there were no obvious defects observed with the atrial or ventricular structures upon *Tie1* deficiency alone at E10.5, while loss of *Tie1* combined with the heterozygous deletion of *Tek* suppressed both atria and ventricle development. White arrows point to the trabecular structures. Quantification of the EMCN-positive area in the ventricular trabeculae at E10.5, and the quantification data of mutant mice was normalized against that of littermate control mice (**B**, LV: *Tie1*$^{\Delta ICD/\Delta ICD}$: 0.86±0.11, n=4; *Control*: 1.00±0.14, n=5; *P*=0.29. RV: *Tie1*$^{\Delta ICD/\Delta ICD}$: 0.79±0.19, n=4; *Control*: 1.00±0.15, n=5; *P*=0.19. **D**, *Tie1*$^{\Delta ICD/\Delta ICD}$*;Tek*$^{+/-}$: 0.64±0.22, n=6; *Control*: 1.00±0.16, n=7; *P*=0.0047). **E**. For the induced gene deletion, tamoxifen intraperitoneal (i.p.) administration (starting from E10.5) and analysis scheme (at E14.5-E16.5). **F**. The deletion efficiency of TIE1 was examined by the immunostaining of skins from *Tie1ICD*^{iECKO}*;Tek*$^{+/-}$ and littermate control mice at E16.5 for PECAM1 (green) and TIE1 (red). **G-H**. Analysis of heart trabeculae of *Tie1ICD*^{iECKO}*;Tek*$^{+/-}$ mice and littermate controls by immunostaining for EMCN (green), PECAM1 (red) and DAPI (blue) at E14.5. Note that the atrial trabeculae structure was missing, while the ventricular trabeculae became sparse (white arrows). Arrows point to the trabecula-associated endocardium. In B and D, statistical analysis was performed using the unpaired nonparametric Mann-Whitney U test. Values are represented as means ± SD of at least three independent technical replicates. LA: left atria, RA: right atria, LV: left ventricle, RV: right ventricle. Scale bar: 200 μm in A(left) and C(left), 30 μm in A(right) and C (right), 400 μm in G, 200 μm in F and 50 μm in H.

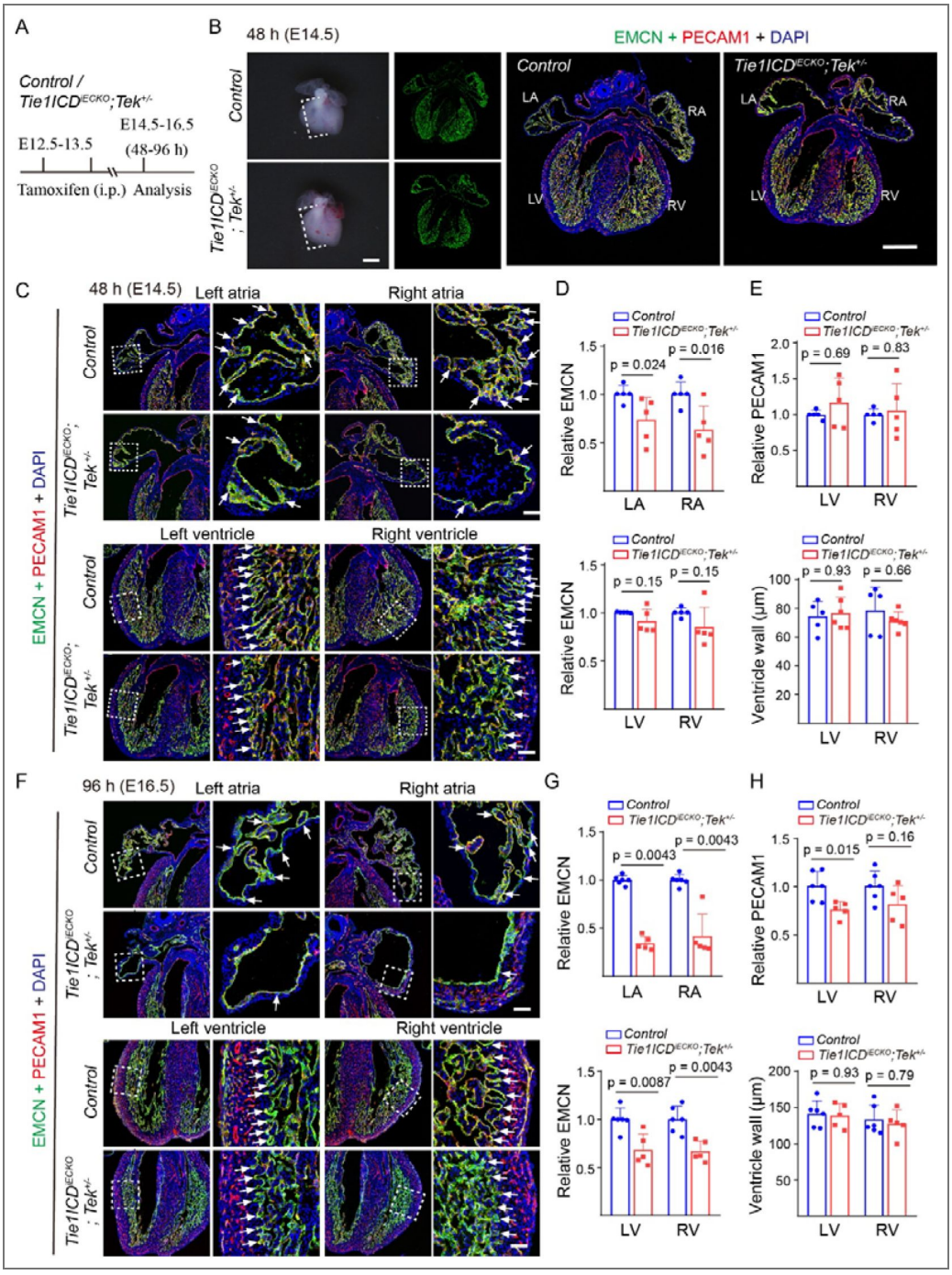

Fig. 6. Synergistic role of TIE1 and TIE2 in the atrial trabeculation.

A. Tamoxifen intraperitoneal (i.p.) administration and analysis scheme. **B-H**. The induced gene deletion by tamoxifen started at E12.5. Analysis of heart trabeculae of *Tie1ICD*^{iECKO}*;Tek*$^{+/-}$and littermate controls by immunostaining for EMCN (green), PECAM1 (red) and DAPI (blue) at E14.5 (**B-C**) and E16.5 (**F**). Note that the atrial trabeculae were absent and the ventricular trabeculae were slightly sparse in the doubly mutant mice at E14.5 (**B-C**), and the phenotype became more severe at E16.5 (**F**). Quantification of the EMCN-positive area in the atrial and ventricular trabeculae (**D**, E14.5; **G**, E16.5), the PECAM1-positive area in ventricular walls and the ventricular wall thickness (**E**, E14.5; **H**, E16.5). Arrows point to the trabecula-associated endocardium. The quantification data of mutant mice was normalized against that of littermate control mice as shown in Table 2 and Table 3. Arrows in C and F point to the trabecula-associated endocardium. In D, E, G and H, statistical analysis was performed using the unpaired nonparametric Mann-Whitney U test. Values are represented as means ± SD of at least three independent technical replicates. LA: left atria, RA: right atria, LV: left ventricle, RV: right ventricle. Scale bar: 400 μm in B, 50 μm in C and F.

Table 2. Quantitation of the trabecular area (EMCN$^+$), blood vessel density in ventricular wall (PECAM1$^+$) and ventricular wall thickness in *Tie1ICD^{iECKO};Tek$^{+/-}$* and littermate controls (at E14.5, 48 hours after the induced gene deletion).

Statistical analysis was performed using the unpaired nonparametric Mann-Whitney U test. Values are represented as means ± SD of at least three independent technical replicates.

		LA	RA	LV	RV
Relative EMCN	*Control* (n=5,mean±sd)	1.00±0.086	1.00±0.12	1.00±0.0050	1.00±0.048
	Tie1ICD^{iECKO};Tek$^{+/-}$ (n=5,mean±sd)	0.73±0.23	0.63±0.24	0.91±0.12	0.85±0.21
	P	0.024	0.016	0.15	0.15
Relative PECAM1	*Control* (n=5,mean±sd)	-	-	1.00±0.060	1.00±0.083
	Tie1ICD^{iECKO};Tek$^{+/-}$ (n=5,mean±sd)	-	-	1.17±0.34	1.06±0.38
	P	-	-	0.69	0.83
Ventricle wall (μm)	*Control* (n=5,mean±sd)	-	-	74.48±10.62	78.56±16.48
	Tie1ICD^{iECKO};Tek$^{+/-}$ (n=6,mean±sd)	-	-	76.87±11.33	71.33±6.25
	P	-	-	0.93	0.66

Table 3. Quantitation of the trabecular area (EMCN$^+$), coronary vessel density in ventricular wall (PECAM1$^+$) and ventricular wall thickness in *Tie1ICD^{iECKO};Tek$^{+/-}$* and littermate controls 96 hours after the induced gene deletion (E16.5; tamoxifen treatment from E12.5-E13.5).

Statistical analysis was performed using the unpaired nonparametric Mann-Whitney U test. Values are represented as means ± SD of at least three independent technical replicates.

		LA	RA	LV	RV
Relative EMCN	*Control* (n=6, mean±sd)	1.00±0.048	1.00±0.059	1.00±0.12	1.00±0.14
	Tie1ICD^{iECKO};Tek$^{+/-}$ (n=5, mean±sd)	0.34±0.069	0.42±0.23	0.68±0.17	0.67±0.11
	P	0.0043	0.0043	0.0087	0.0043
Relative PECAM1	*Control* (n=6,mean±sd)	-	-	1.00±0.15	1.00±0.16
	Tie1ICD^{iECKO};Tek$^{+/-}$ (n=5, mean±sd)	-	-	0.76±0.083	0.81±0.19
	P	-	-	0.015	0.16
Ventricle wall (μm)	*Control* (n=6, mean±sd)	-	-	141.45±18.02	133.36±20.44
	Tie1ICD^{iECKO};Tek$^{+/-}$ (n=5, mean±sd)	-	-	138.90±16.66	127.81±18.81
	P	-	-	0.93	0.79

weight (Fig. 7 F, G), and showed abnormal atrial trabeculation while the trabeculae in the ventricles had no obvious defects (Fig. 7F, H). There was a significant decrease of trabecular structures (white arrows in Fig. 7H) in atria of *Tie1ICD*^{iECKO}*; Tek*$^{+/-}$ mice compare with that of the control mice (LA, *Tie1ICD*^{iECKO}*; Tek*$^{+/-}$: 0.69±0.16, n=11; *Control*: 1.00±0.28, n=16; *P*=0.0022. RA, *Tie1ICD*^{iECKO}*; Tek*$^{+/-}$: 0.77±0.15, n=11; *Control*: 1.00±0.11, n=16; *P*=0.0002). The effects of TIE1 and TIE2 deficiency or insufficiency on heart trabecular morphogenesis were summarized in Fig. 7I. Based on the previous findings about the TIE1/TIE2 in venous EC specification [28,30], we propose that TIE1 acts in synergy with TIE2 in the specification of atrial endocardial cells (Fig. 7I). TIE1 deficiency or TIE1/TIE2 insufficiency results in a more severe defects with the atrial trabeculation, suggesting the differential requirement of TIE1 and TIE2 in the endocardium-mediated organization of the atrial internal muscular network.

Discussion

Developmental defects or pathological remodeling of atria may result in the atrial dysfunction leading to the heart failure [43]. In contrast to the better understanding of ventricular chamber morphogenesis, the dynamic process and regulatory networks of the atrial internal muscular network formation (known as atrial trabeculation) are inadequately elucidated. TIE1 variants or loss of function mutations were reported in a subset of lymphedema patients [34,35], and it is unknown whether the patients have also cardiac defects in addition to the lymphatic abnormality. We show in this study that the atrial trabeculation occurred later than in ventricles. Based on the analysis of the published scRNA-seq data by Feng et al. [36] and the bulk RNA-seq analysis of atria and ventricles separately in this study, we showed that *Tie1* and its homologue *Tek* were highly expressed in atrial endocardial cells than those of ventricles. By employing the genetically modified mouse models targeting *Tie1*, *Tek* and both, we found that TIE1 was differentially required in the process of atrial versus ventricular trabeculation and acted in synergy with TIE2 in the process of cardiac trabeculation, especially in atria.

Endocardial versus vascular effects of TIE1

Cardiac chamber morphogenesis involves the coordinated endocardial-myocardial interaction governed by a plethora of cardiovascular regulators [2]. It is worth noting that most of the reported endothelial regulators have important roles in both heart and vascular development. ANGPT1 has been shown to participate in the regulation of atria and cardiac vein development [19,44]. We have demonstrated that TIE1 and TIE2 are required for the vein specification via regulating the protein stability of COUPTFII [30]. Disruption of COUPTFII led to the defective atrial and venous formation [31,33]. Defective cardiac venous formation was also observed in this study in *Tie1* or *Tek* mutant mice at later embryonic stages. It is therefore important to dissect whether cardiac defects in the mutants are a direct effect or secondary to the coronary vascular defects. By performing a serial analysis of the developing hearts during embryogenesis (including E10.5, E12,5, E14.5, E16.5, E17.5), we found in this study that TIE1 deficiency resulted in an impaired atrial trabeculation readily detectable at embryonic day 12.5 (E12.5), while there were only minor defects observed with the ventricular trabeculae at the same stage. In addition, *Tek* deficiency leads to the embryonic lethality before E10.5 [30,45]. Interestingly, the defective atrial trabeculae formation was detected within 48 hours after the induced deletion of endothelial *Tek* (starting from E12.5), while there were no obvious defects with coronary vessels at the same stage. This was further confirmed in the *Tie1/Tek* doubly mutant mice with defective atrial trabeculation detected within 48 hours after the induced deletion of *Tie1* combined with one null allele of *Tek*. Lack of TIE1 did not produce obvious developmental defects in mutant embryos by E10.5 as previously reported [26,28]. Therefore, the differential requirement of TIE1 may be related to the specification of atrial versus ventricular endocardium, which involves a synergistic role of TIE2, as previously reported in vein development [28,30]. Based on the above findings, it is likely that TIE1 and TIE2 are directly required for the endocardial cell-mediated organization of atrial trabecular structures. In addition, defects with the ventricular trabeculation and a trend of thinner ventricle walls were also observed at later stages after the *Tie1* deficiency or induced *Tie1/Tek* insufficiency. The cardiac trabeculation

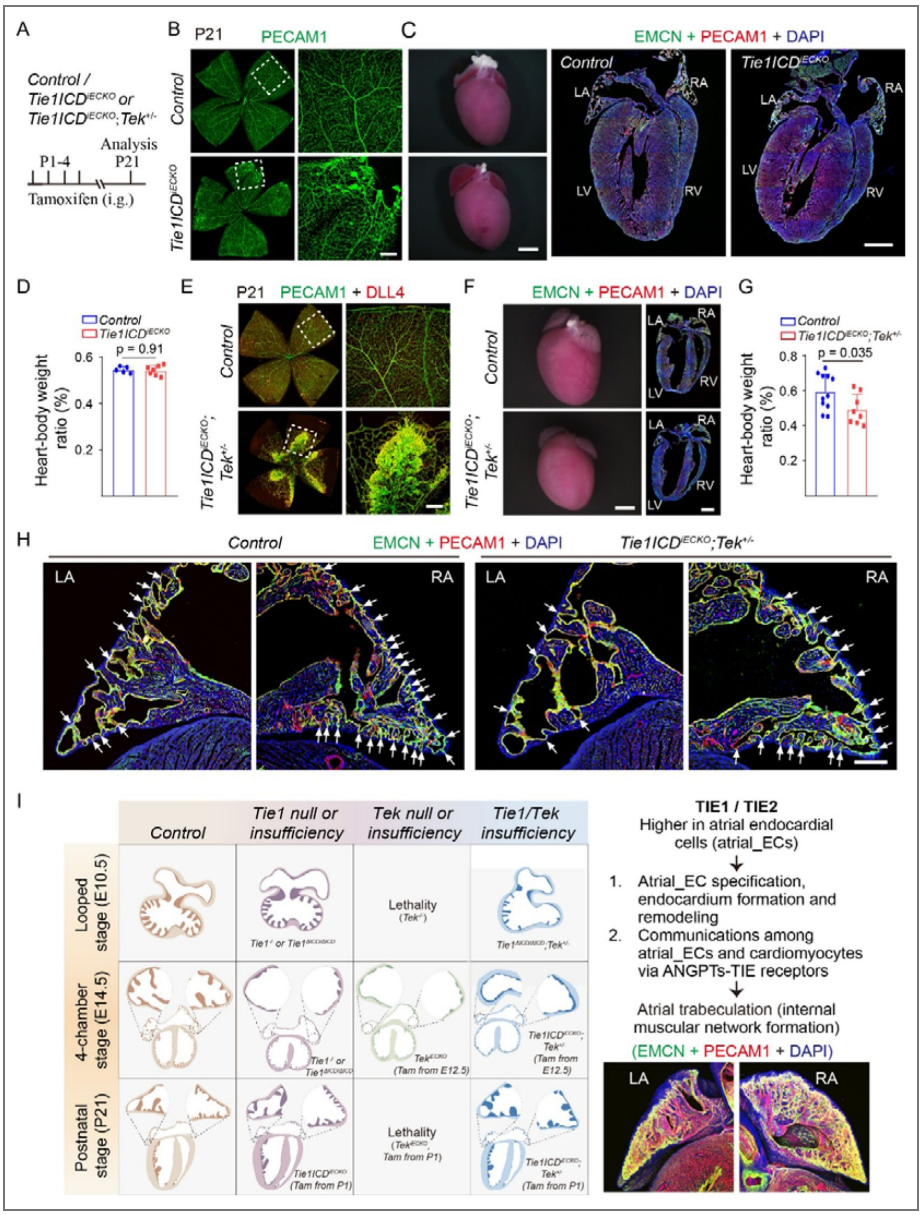

Fig. 7. Abnormal atrial trabecular remodeling after the postnatal deletion of *Tie1* combined with one null allele of *Tek*.

A. Tamoxifen intragastric (i.g.) administration and the analysis scheme. **B-H**. Analysis of blood vessels in the retinas of *Tie1ICD*^{iECKO} (**B**), *Tie1ICD*^{iECKO}*;Tek*$^{+/-}$(**E**) and *control* mice by whole-mount immunostaining for PECAM1 (green), DLL4 (red) at P21. Note that hemangioma-like vascular tufts observed in *Tie1ICD*^{iECKO} and *Tie1ICD*^{iECKO}*;Tek*$^{+/-}$mice. The retinal vascular defects were used to confirm the efficiency of induced gene deletion. Analysis of heart trabeculae in *Tie1ICD*^{iECKO} (**C**), *Tie1ICD*^{iECKO}*;Tek*$^{+/-}$(**F**) and control mice by the immunostaining for EMCN (green), PECAM1 (red) and DAPI (blue) at P21. TIE1 insufficiency alone had no obvious effect on heart size (**D**, *Tie1ICD*^{iECKO}: 0.54±0.021, n=7; *Control*: 0.54±0.014, n=5; *P*=0.91.) and atrial trabecular structures (**C**). The *Tie1ICD*^{iECKO}*;Tek*$^{+/-}$ mice displayed smaller hearts (**G**, *Tie1ICD*^{iECKO}*;Tek*$^{+/-}$: 0.49±0.086, n=8; *Control*: 0.59±0.10, n=11; *P*=0.035.) and abnormal atrial trabecular morphology (**F**,**H**). White arrows in H point to the trabecula-associated endocardium in the atria. **I**. Schematic illustration of TIE1, TIE2 and their synergy in cardiac chamber morphogenesis. TIE1 deficiency, TIE2 or TIE1/TIE2 insufficiency results in a more severe defect with the atrial trabeculation than that of ventricles. Based on the previous findings about the TIE1/TIE2 in venous EC specification [28,30] and findings from this study, we propose that TIE1 acts in synergy with TIE2 in the specification and remodeling of atrial endocardium, and that there is a differential requirement of TIE receptors in atrial versus ventricular wall morphogenesis. In D and G, statistical analysis was performed using the unpaired nonparametric Mann-Whitney U test (D) and the unpaired t test (G). Values are represented as means ± SD of at least three independent technical replicates. Scale bar: 50 μm in B and E, 1 mm in C and F, 200 μm in H.

contributes to the thickening and maturation of the ventricular wall by being incorporated into the compact myocardium [4,8]. It has been reported that endocardial cells contribute to the formation of coronary vascular network formation [10]. The defective ventricular wall morphogenesis may also be related to the decreased coronary vessel growth in Tie1 or *Tie1/Tek* mutant mice as observed in this study.

Synergy of TIE1 and TIE2 in cardiac trabeculation

Loss of TIE1 alone did not produce an obvious defect with atrial chamber formation at initial stages of heart development (e.g. E10.5). However, the loss of *Tie1* combined with the heterozygous deletion of *Tek* disrupted the atrial and ventricle development at the same stage (E10.5). The synergy of TIE1 and TIE2 in heart development was further verified at later embryogenesis as well as the postnatal studies. The defects with the atrial trabeculation were already detectable 48 hours later in the induced knockout of *Tie1* plus the heterzygous *Tek* deletion (starting at E12.5, $Tie1ICD^{iECKO}$; $Tek^{+/-}$). This was further confirmed at the neonatal with the induced gene deletion from postnatal day 1 and the analysis 3-weeks later stage ($Tie1ICD^{iECKO}$; $Tek^{+/-}$), while TIE1 insufficiency alone ($Tie1ICD^{iECKO}$) had no obvious impact on the atrial or ventricular trabecula development. TIE1 and TIE2 could form heterodimers, participate in the formation of endothelial cell-cell adherens junction as well as the EC migration and survival [21,22,46,47]. Furthermore, TIE1 and TIE2 act in a synergistic manner to specify the vein formation via regulating the protein stability of the venous factor COUPTFII [28,30]. As COUPTFII is crucial for the atrial development [31,33], this could provide some insights into the synergy of TIE1/TIE2 in the regulation of cardiac trabeculation especially in atria, likely involving COUPTFII-mediated regulation of the atrial endocardial cell specification.

Differential requirement of TIE receptors in atria and ventricles

So far, little is known about mechanisms underlying the differential regulation of atrial versus ventricular endocardial development. We found in this study that *Tie1* and *Tek* were expressed at higher levels in atrial endocardial cells than those of ventricles by the RNA-seq analysis at the single cell level or the separate analysis of atria and ventricles. By the analysis of scRNA-seq data from embryonic hearts for the ligand-receptor interactions, we showed that the atrial endocardial cells and cardiomyocytes exhibited stronger ANGPT1-TIE2 signaling compared with those in ventricles. This suggests that the differential requirement of TIE1 and TIE2 in cardiac chamber morphogenesis may, at least partly, be related to the differential expression levels of TIE receptors in atrial versus ventricular endocardial cells. In addition, we also found that *Dll1* was mainly expressed by endocardial cells from the analysis of single cell RNA-seq data [36], and that *Dll1* was among the most downregulated genes in the hearts from *Tie1* deficient mice. A similar trend of decreased expression with *Notch1* was also detected in atria but not in ventricles of *Tie1* deficient mice. As NOTCH1 signaling promotes the extracellular matrix degradation during the formation of endocardial projections that are critical for individualization of trabecular units [13,15], this may also contribute to the differential requirement of TIE1 as well as TIE2 in atrial versus ventricular trabeculation.

In summary, findings from this study show that endothelial TIE1 is crucial for the atrial trabecular formation and play synergistic roles with TIE2 in the process of cardiac chamber morphogenesis. *Tie1* deficiency resulted in the significant decrease of *Tek*, *Dll1* and *Notch1*. This suggests that the differential requirement of TIE receptors in the process of atrial and ventricular trabeculation may involve the DLL1-NOTCH1 pathway. Mechanisms underlying the differential regulation of atrial versus ventricular formation during the heart development warrants further investigation. Knowledge in this direction will facilitate the development of novel interventions for the atria-related cardiomyopathy.

Data availability

RNA sequence data will be deposited in GEO and information provided later.

Acknowledgements

The authors thank the staff in Animal facility of Soochow University for technical assistance.

Additional information

Funding

This work was supported by grants from the National Key R&D Program of China (2021YFA0805000), the National Natural Science Foundation of China (82470518, 82401544), China Postdoctoral Science Foundation (CPSF, 2024M762300), the Natural Science Foundation of Jiangsu Province (BK20240786), the Project of State Key Laboratory of Radiation Medicine and Protection (No. GZN120 20 02), and the Priority Academic Program Development of Jiangsu Higher Education Institutions.

Funding

Funder	Grant reference number	Author
MOST | National Key Research and Development Program of China (NKPs)	2021YFA0805000	Yulong He
MOST | National Natural Science Foundation of China (NSFC)	82470518	Yulong He
MOST | National Natural Science Foundation of China (NSFC)	82401544	Xudong Cao
China Postdoctoral Science Foundation	2024M762300	Taotao Li
JST | Natural Science Foundation of Jiangsu Province (Jiangsu Natural Science Foundation)	BK20240786	Xudong Cao
Project of State Key Laboratory of Radiation Medicine and Protection	GZN120 20 02	Yulong He
Priority Academic Program Development of Jiangsu Higher Education Institutions (PAPD)		Yulong He

Author ORCID iDs

Kai Ding: https://orcid.org/0009-0008-1443-0163
Beibei Xu: https://orcid.org/0009-0000-0861-5593
Zhen Zhang: https://orcid.org/0000-0002-9898-054X
Yulong He: https://orcid.org/0000-0002-0099-3749

Additional files

Supplemental Figures and Tables

Supplemental Figure 6 for Fig. 3A Control

Supplemental Figure 6 for Fig. 3A Tie1tm1a

References

1. **Meilhac SM,** Buckingham ME (2018) The deployment of cell lineages that form the mammalian heart. *Nat Rev Cardiol* **15**:705-724 https://doi.org/10.1038/s41569-018-0086-9 | PubMed
2. **Tian Y,** Morrisey EE (2012) Importance of myocyte-nonmyocyte interactions in cardiac development and disease. *Circ Res* **110**:1023-1034 https://doi.org/10.1161/CIRCRESAHA.111.243899 | PubMed
3. **Moorman AF,** Christoffels VM (2003) Cardiac chamber formation: development, genes, and evolution. *Physiol Rev* **83**:1223-1267 https://doi.org/10.1152/physrev.00006.2003 | PubMed

4. **Tran YTH,** Saha D, Del Monte-Nieto G (2025) Cardiac trabeculation in vertebrates: Convergent evolution or evolutionary adaptations associated with heart complexity?. *Seminars in cell & developmental biology* **172** https://doi.org/10.1016/j.semcdb.2025.103622 | PubMed
5. **Haack T,** Abdelilah-Seyfried S (2016) The force within: endocardial development, mechanotransduction and signalling during cardiac morphogenesis. *Development* **143**:373-386 https://doi.org/10.1242/dev.131425 | PubMed
6. **Rhee S,** Paik DT, Yang JY, Nagelberg D, Williams I, Tian L, Roth R, Chandy M, Ban J, Belbachir N, *et al.* (2021) Endocardial/endothelial angiocrines regulate cardiomyocyte development and maturation and induce features of ventricular non-compaction. *Eur Heart J* **42**:4264-4276 https://doi.org/10.1093/eurheartj/ehab298 | PubMed
7. **Captur G,** Syrris P, Obianyo C, Limongelli G, Moon JC (2015) Formation and Malformation of Cardiac Trabeculae: Biological Basis, Clinical Significance, and Special Yield of Magnetic Resonance Imaging in Assessment. *The Canadian journal of cardiology* **31**:1325-1337 https://doi.org/10.1016/j.cjca.2015.07.003 | PubMed
8. **Gunawan F,** Priya R, Stainier DYR (2021) Sculpting the heart: Cellular mechanisms shaping valves and trabeculae. *Current opinion in cell biology* **73**:26-34 https://doi.org/10.1016/j.ceb.2021.04.009 | PubMed
9. **Samsa LA,** Yang B, Liu J (2013) Embryonic cardiac chamber maturation: Trabeculation, conduction, and cardiomyocyte proliferation. *Am J Med Genet C Semin Med Genet* 157-168 https://doi.org/10.1002/ajmg.c.31366 | PubMed
10. **Meilhac SM,** Buckingham ME (2018) The deployment of cell lineages that form the mammalian heart. *Nature reviews Cardiology* **15**:705-724 https://doi.org/10.1038/s41569-018-0086-9 | PubMed
11. **Wu B,** Zhang Z, Lui W, Chen X, Wang Y, Chamberlain AA, Moreno-Rodriguez RA, Markwald RR, O'Rourke BP, Sharp DJ, *et al.* (2012) Endocardial cells form the coronary arteries by angiogenesis through myocardial-endocardial VEGF signaling. *Cell* **151**:1083-1096 https://doi.org/10.1016/j.cell.2012.10.023 | PubMed
12. **Lai D,** Liu X, Forrai A, Wolstein O, Michalicek J, Ahmed I, Garratt AN, Birchmeier C, Zhou M, Hartley L, *et al.* (2010) Neuregulin 1 sustains the gene regulatory network in both trabecular and nontrabecular myocardium. *Circ Res* **107**:715-727 https://doi.org/10.1161/CIRCRESAHA.110.218693 | PubMed
13. **Grego-Bessa J,** Luna-Zurita L, del Monte G, Bolos V, Melgar P, Arandilla A, Garratt AN, Zang H, Mukouyama YS, Chen H, *et al.* (2007) Notch signaling is essential for ventricular chamber development. *Dev Cell* **12**:415-429 https://doi.org/10.1016/j.devcel.2006.12.011 | PubMed
14. **Watanabe Y,** Kokubo H, Miyagawa-Tomita S, Endo M, Igarashi K, Aisaki K, Kanno J, Saga Y (2006) Activation of Notch1 signaling in cardiogenic mesoderm induces abnormal heart morphogenesis in mouse. *Development* **133**:1625-1634 https://doi.org/10.1242/dev.02344 | PubMed
15. **Del Monte-Nieto G,** Ramialison M, Adam AAS, Wu B, Aharonov A, D'Uva G, Bourke LM, Pitulescu ME, Chen H, de la Pompa JL, *et al.* (2018) Control of cardiac jelly dynamics by NOTCH1 and NRG1 defines the building plan for trabeculation. *Nature* **557**:439-445 https://doi.org/10.1038/s41586-018-0110-6 | PubMed
16. **Miao L,** Lu Y, Nusrat A, Fan G, Zhang S, Zhao L, Wu CL, Guo H, Huyen TLN, Zheng Y, *et al.* (2025) Tunneling nanotube-like structures regulate distant cellular interactions during heart formation. *Science* **387**:eadd3417 https://doi.org/10.1126/science.add3417 | PubMed
17. **Lockhart M,** Wirrig E, Phelps A, Wessels A (2011) Extracellular matrix and heart development. *Birth Defects Res A Clin Mol Teratol* **91**:535-550 https://doi.org/10.1002/bdra.20810 | PubMed
18. **Kern CB,** Wessels A, McGarity J, Dixon LJ, Alston E, Argraves WS, Geeting D, Nelson CM, Menick DR, Apte SS (2010) Reduced versican cleavage due to Adamts9 haploinsufficiency is associated with cardiac and aortic anomalies. *Matrix biology : journal of the International Society for Matrix Biology* **29**:304-316 https://doi.org/10.1016/j.matbio.2010.01.005 | PubMed

19. **Kim KH,** Nakaoka Y, Augustin HG, Koh GY (2018) Myocardial Angiopoietin-1 Controls Atrial Chamber Morphogenesis by Spatiotemporal Degradation of Cardiac Jelly. *Cell Rep* **23**:2455-2466 https://doi.org/10.1016/j.celrep.2018.04.080 | PubMed

20. **Qu X,** Harmelink C, Baldwin HS (2019) Tie2 regulates endocardial sprouting and myocardial trabeculation. *JCI Insight* **5** https://doi.org/10.1172/jci.insight.96002 | PubMed

21. **Augustin HG,** Koh GY, Thurston G, Alitalo K (2009) Control of vascular morphogenesis and homeostasis through the angiopoietin-Tie system. *Nature reviews Molecular cell biology* **10**:165-177 https://doi.org/10.1038/nrm2639 | PubMed

22. **Saharinen P,** Eklund L, Alitalo K (2017) Therapeutic targeting of the angiopoietin-TIE pathway. *Nature reviews Drug discovery* **16**:635-661 https://doi.org/10.1038/nrd.2016.278 | PubMed

23. **Qu X,** Harmelink C, Baldwin HS (2019) Tie2 regulates endocardial sprouting and myocardial trabeculation. *JCI Insight* **5** https://doi.org/10.1172/jci.insight.96002 | PubMed

24. **Leppanen VM,** Saharinen P, Alitalo K (2017) Structural basis of Tie2 activation and Tie2/Tie1 heterodimerization. *Proc Natl Acad Sci U S A* **114**:4376-4381 https://doi.org/10.1073/pnas.1616166114 | PubMed

25. **Puri MC,** Rossant J, Alitalo K, Bernstein A, Partanen J (1995) The receptor tyrosine kinase TIE is required for integrity and survival of vascular endothelial cells. *The EMBO journal* **14**:5884-5891 https://doi.org/10.1002/j.1460-2075.1995.tb00276.x | PubMed

26. **Shen B,** Shang Z, Wang B, Zhang L, Zhou F, Li T, Chu M, Jiang H, Wang Y, Qiao T, *et al.* (2014) Genetic dissection of tie pathway in mouse lymphatic maturation and valve development. *Arterioscler Thromb Vasc Biol* **34**:1221-1230 https://doi.org/10.1161/ATVBAHA.113.302923 | PubMed

27. **Qu X,** Tompkins K, Batts LE, Puri M, Baldwin S (2010) Abnormal embryonic lymphatic vessel development in Tie1 hypomorphic mice. *Development* **137**:1285-1295 https://doi.org/10.1242/dev.043380 | PubMed

28. **Cao X,** Li T, Xu B, Ding K, Li W, Shen B, Chu M, Zhu D, Rui L, Shang Z, *et al.* (2023) Endothelial TIE1 Restricts Angiogenic Sprouting to Coordinate Vein Assembly in Synergy With Its Homologue TIE2. *Arterioscler Thromb Vasc Biol* **43**:e323-e338 https://doi.org/10.1161/ATVBAHA.122.318860 | PubMed

29. **Qu X,** Violette K, Sewell-Loftin MK, Soslow J, Saint-Jean L, Hinton RB, Merryman WD, Baldwin HS (2019) Loss of flow responsive Tie1 results in ImpairedAortic valve remodeling. *Dev Biol* https://doi.org/10.1016/j.ydbio.2019.07.011 | PubMed

30. **Chu M,** Li T, Shen B, Cao X, Zhong H, Zhang L, Zhou F, Ma W, Jiang H, Xie P, *et al.* (2016) Angiopoietin receptor Tie2 is required for vein specification and maintenance via regulating COUP-TFII. *eLife* **5**:e21032 https://doi.org/10.7554/eLife.21032 | PubMed

31. **Pereira FA,** Qiu Y, Zhou G, Tsai MJ, Tsai SY (1999) The orphan nuclear receptor COUP-TFII is required for angiogenesis and heart development. *Genes Dev* **13**:1037-1049 https://doi.org/10.1101/gad.13.8.1037 | PubMed

32. **You LR,** Lin FJ, Lee CT, DeMayo FJ, Tsai MJ, Tsai SY (2005) Suppression of Notch signalling by the COUP-TFII transcription factor regulates vein identity. *Nature* **435**:98-104 https://doi.org/10.1038/nature03511 | PubMed

33. **Wu SP,** Cheng CM, Lanz RB, Wang T, Respress JL, Ather S, Chen W, Tsai SJ, Wehrens XH, Tsai MJ, *et al.* (2013) Atrial identity is determined by a COUP-TFII regulatory network. *Dev Cell* **25**:417-426 https://doi.org/10.1016/j.devcel.2013.04.017 | PubMed

34. **Michelini S,** Ricci M, Veselenyiova D, Kenanoglu S, Kurti D, Baglivo M, Fiorentino A, Basha SH, Priya S, Serrani R, *et al.* (2020) TIE1 as a Candidate Gene for Lymphatic Malformations with or without Lymphedema. *International journal of molecular sciences* **21** https://doi.org/10.3390/ijms21186780 | PubMed

35. **Brouillard P,** Murtomaki A, Leppanen VM, Hyytiainen M, Mestre S, Potier L, Boon LM, Revencu N, Greene A, Anisimov A, *et al.* (2024) Loss-of-function mutations of the TIE1 receptor tyrosine kinase cause late-onset primary lymphedema. *J Clin Invest* **134** https://doi.org/10.1172/JCI173586 | PubMed

36. **Feng W,** Bais A, He H, Rios C, Jiang S, Xu J, Chang C, Kostka D, Li G (2022) Single-cell transcriptomic analysis identifies murine heart molecular features at embryonic and neonatal stages. *Nature communications* **13**:7960 https://doi.org/10.1038/s41467-022-35691-7 | PubMed

37. **Shen B,** Shang Z, Wang B, Zhang LQ, Zhou F, Li TT, Chu M, Jiang HJ, Wang Y, Qiao T, *et al.* (2014) Genetic Dissection of Tie Pathway in Mouse Lymphatic Maturation and Valve Development. *Arterioscl Throm Vas* **34**:1221-1230 https://doi.org/10.1161/Atvbaha.113.302923 | PubMed

38. **Chu M,** Li TT, Shen B, Cao XD, Zhong HY, Zhang LQ, Zhou F, Ma WJ, Jiang HJ, Xie PC, *et al.* (2016) Angiopoietin receptor Tie2 is required for vein specification and maintenance via regulating COUP-TFII. *eLife* **5** https://doi.org/10.7554/eLife.21032 | PubMed

39. **Okabe K,** Kobayashi S, Yamada T, Kurihara T, Tai-Nagara I, Miyamoto T, Mukouyama YS, Sato TN, Suda T, Ema M, *et al.* (2014) Neurons limit angiogenesis by titrating VEGF in retina. *Cell* **159**:584-596 https://doi.org/10.1016/j.cell.2014.09.025 | PubMed

40. **Cao X,** Xu B, Li X, Li T, He Y (2021) A Genetically Engineered Mouse Model of Venous Anomaly and Retinal Angioma-like Vascular Malformation. *Bio Protoc* **11**:e4117 https://doi.org/10.21769/BioProtoc.4117 | PubMed

41. **Kalucka J,** de Rooij L, Goveia J, Rohlenova K, Dumas SJ, Meta E, Conchinha NV, Taverna F, Teuwen LA, Veys K, *et al.* (2020) Single-Cell Transcriptome Atlas of Murine Endothelial Cells. *Cell* **180**:764-779.e720. https://doi.org/10.1016/j.cell.2020.01.015 | PubMed

42. **Liberzon A,** Birger C, Thorvaldsdottir H, Ghandi M, Mesirov JP, Tamayo P (2015) The Molecular Signatures Database (MSigDB) hallmark gene set collection. *Cell Syst* **1**:417-425 https://doi.org/10.1016/j.cels.2015.12.004 | PubMed

43. **Fatkin D,** Huttner IG, Johnson R (2019) Genetics of atrial cardiomyopathy. *Current opinion in cardiology* **34**:275-281 https://doi.org/10.1097/HCO.0000000000000610 | PubMed

44. **Arita Y,** Nakaoka Y, Matsunaga T, Kidoya H, Yamamizu K, Arima Y, Kataoka-Hashimoto T, Ikeoka K, Yasui T, Masaki T, *et al.* (2014) Myocardium-derived angiopoietin-1 is essential for coronary vein formation in the developing heart. *Nature communications* **5**:4552 https://doi.org/10.1038/ncomms5552 | PubMed

45. **Sato TN,** Tozawa Y, Deutsch U, Wolburg-Buchholz K, Fujiwara Y, Gendron-Maguire M, Gridley T, Wolburg H, Risau W, Qin Y (1995) Distinct roles of the receptor tyrosine kinases Tie-1 and Tie-2 in blood vessel formation. *Nature* **376**:70-74 https://doi.org/10.1038/376070a0 | PubMed

46. **Saharinen P,** Eklund L, Miettinen J, Wirkkala R, Anisimov A, Winderlich M, Nottebaum A, Vestweber D, Deutsch U, Koh GY, *et al.* (2008) Angiopoietins assemble distinct Tie2 signalling complexes in endothelial cell-cell and cell-matrix contacts. *Nat Cell Biol* **10**:527-537 https://doi.org/10.1038/ncb1715 | PubMed

47. **Fukuhara S,** Sako K, Minami T, Noda K, Kim HZ, Kodama T, Shibuya M, Takakura N, Koh GY, Mochizuki N (2008) Differential function of Tie2 at cell-cell contacts and cell-substratum contacts regulated by angiopoietin-1. *Nat Cell Biol* **10**:513-526 https://doi.org/10.1038/ncb1714 | PubMed

Peer reviews

Reviewer #1 (Public review):

Summary:

In this manuscript, Ding et al. use genetic mouse models to demonstrate that atrial trabeculation is more dependent on Tie1/Tie2 signaling than ventricular trabeculation. With additional experimentation that would support the current claims, the results may hold significant value, as atrial trabeculation remains an understudied phenomenon in cardiac biology with potential implications for atrial cardiomyopathy and atrial fibrillation.

Strengths:

Detailed characterization of atrial versus ventricular trabeculation across different developmental timepoints, and the use of appropriate animal models to address the scientific question at hand.

Weaknesses:

The authors have consistently treated mice with tamoxifen after ventricular, but not atrial, trabeculation has already started. As such, the observed cardiac phenotypes - where predominantly atrial trabeculation is affected - might be a mere consequence of the precise time window in which Tie1/2 signaling was impaired, rather than a direct measurement of its relative importance for atrial versus ventricular trabeculation. The conclusions of the paper may thus be significantly strengthened by depleting Tie1/2 signaling prior to the onset of ventricular trabeculation, as is done for atrial trabeculation.

https://doi.org/10.7554/eLife.111156.1.sa3

Reviewer #2 (Public review):

Summary:

Ding et al. examine the role of TIE1 in cardiac chamber morphogenesis using genetic mouse models targeting Tie1, Tek, or both, and analyzing endocardial cell-mediated chamber formation across multiple embryonic developmental and postnatal stages, supported by analysis of published single-cell datasets and new bulk RNA seq analyses of murine cardiac tissue. The authors find that Tie1 and Tek expression is higher in atrial than ventricular endocardial cells. Notably, endothelial Tie1 is required for atrial trabeculation at E12.5, but is less critical in ventricular trabeculation. TIE1 also acts synergistically with TIE2 during atrial trabeculation. While Tie1 deficiency alone does not cause defects at E10.5, combined heterozygous deletion of Tek disrupts both atrial and ventricular development at E10.5. This synergy is further supported by analyses at later embryonic stages and in postnatal hearts.

Strengths:

The study is well-designed, clearly written, and supported by high-quality figures. The performed experiments demonstrate a previously unrecognized role for Tie1 in cardiac development and identify synergistic control of cardiac morphogenesis by Tie1 and Tie2. This synergy is consistent with the previously identified roles of Tie1 and Tek in venous development and with Tie1 involvement in angiopoietin-dependent postnatal vascular and lymphatic remodeling. Together, these findings support a role for Tie1 as a contributor to Ang1-Tie2 signaling during heart development.

Weaknesses:

The manuscript does not include direct mechanistic studies; however, RNA seq analysis of atria and ventricles showed reduced expression of Tek, Dll1, and Notch1 upon Tie1 deficiency in developing hearts. Although previously reported mechanisms, such as TIE1-TIE2 heterodimer formation and effects on endothelial junctions, migration, or survival are discussed, no direct mechanistic experiments are performed. Addressing some of these mechanisms would have clarified the basis of Tie1-Tie2 synergy. As two distinct Tie1 models are used, including one targeting the kinase domain, the authors should state whether phenotypes differed or were similar between models.

https://doi.org/10.7554/eLife.111156.1.sa2

Reviewer #3 (Public review):

Summary:

Ding et al. investigate the roles of TIE1 and TEK (Tie2) in mouse cardiac development, with a particular focus on atrial trabeculation. The authors employ multiple genetic models, including Tie1ICDflox/flox (with Cdh5-CreERT2), a knockout-first allele (EUCOMM, Tie1 tm1a/tm1a), and a Tek deletion model.

Based on the dataset from Feng et al. 2022 Nat Commun, the authors report increased expression of Tie1 and Tek transcripts in atrial endocardial cells compared to ventricular cells at embryonic day (E) 14.5. Loss of Tie1 leads to early atrial trabeculation defects detectable at E12.5, whereas ventricular defects appear later and are less pronounced at E14.5. Chamber-specific RNA sequencing reveals stronger transcriptional changes in atrial tissue.

Conditional deletion of Tek results in a similar phenotype, with more pronounced atrial defects. Combined deletion of Tie1 and Tek (Tie1 ΔICD/ΔICD; Tek+/-) leads to earlier and more severe defects in both atrial and ventricular trabeculation and results in embryonic lethality around E12.5, suggesting a synergistic interaction between the two genes.

Conditional endothelial deletion of Tie1 combined with heterozygous global Tek at later embryonic stages allows analysis at later time points and again shows more severe defects in atrial trabeculation. Postnatal analysis of this model reveals reduced heart-to-body weight ratios and potential mild atrial abnormalities.

Strengths:

(1) The authors address chamber-specific signaling mechanisms underlying atrial versus ventricular trabeculation, an area of high developmental and clinical relevance.

(2) The study provides a comprehensive temporal analysis across multiple embryonic stages.

(3) The use of multiple genetic models strengthens the overall conclusions and allows comparative interpretation.

(4) While focusing on trabeculation, the authors also include observations on coronary vessel development, increasing the broader relevance of the work. The findings are therefore of interest to the wider cardiovascular research community.

Weaknesses:

(1) Timing of recombination vs. trabeculation onset

Ventricular trabeculation begins earlier than atrial trabeculation. Since tamoxifen (in contrast to 4-hydroxytamoxifen) requires metabolic activation, Cre-mediated recombination will occur with a delay. This suggests that atrial trabeculation may be targeted before its onset, whereas ventricular trabeculation may already be underway for 2-3 days at the time of effective gene deletion.

How do the authors account for this discrepancy in their interpretation?

Have earlier induction time points been tested to better capture the onset of ventricular trabeculation? This limitation should be explicitly discussed.

(2) Clarity of genetic models and experimental design

The study employs several genetic constructs. It would improve clarity if, for each experiment, the specific genetic model and tamoxifen regimen were clearly described before presenting the results.

(3) Tie1 tm1a/tm1a phenotype vs. known global knockout

Previous studies (PMID: 8846781, 7596437) show that complete Tie1 loss leads to severe edema, vascular rupture, and embryonic lethality around E13.5-E14.5.

How does the Tie1 tm1a/tm1a allele differ, given that animals appear to survive longer? Is this allele hypomorphic rather than a full knockout?

This point requires clarification.

(4) Limited mechanistic insight

While the authors aim to investigate underlying mechanisms, the current study is largely descriptive and based on mRNA expression and genetic interaction analyses (Tie1/Tek co-deletion). Direct mechanistic insights into signaling pathways remain limited. However, the dataset provides a valuable foundation for future mechanistic studies, which should be more clearly acknowledged in the discussion.

https://doi.org/10.7554/eLife.111156.1.sa1

Author response:

> ***eLife Assessment***
>
> *This study reports the relative importance of Tie1 and Tie2 signaling for atrial versus ventricular trabeculation. It is an important study and is one of the few works to date that have carefully and simultaneously analyzed these two processes. In line with a previous study in zebrafish, the authors demonstrate key differences between atrial and ventricular trabeculation. While the imaging and quantitative data were conducted with solid and validated methodology throughout the manuscript, the work would benefit from more rigourous approaches where Tie1/2 signaling is disrupted prior to the onset of atrial/ventricular trabeculation, to allow for a more direct comparison.*

We thank the editors for the eLife assessment. We would like to request that the following statement be modified: "…the work would benefit from more rigourous approaches where Tie1/2 signaling is disrupted prior to the onset of atrial/ventricular trabeculation, to allow for a more direct comparison". We request this change for the following reasons:

We utilized two distinct genetic mouse models in this study (as summarized in Fig. 7I), comprising conventional knockouts (*Tie1*$^{tm1a/tm1a}$, *Tie1*$^{\Delta ICD/\Delta ICD}$ and *Tie1*$^{\Delta ICD/\Delta ICD}$;*Tek*$^{+/-}$) and inducible gene deletion models (*Tek*^{iECKO}, *Tie1ICD*^{iECKO}, and *Tie1ICD*^{iECKO};*Tek*$^{+/-}$) [1-3]. The *Tie1*$^{tm1a/tm1a}$ line is equivalent to the previously published *Tie1*$^{-/-</sup}$ mouse line, as demonstrated in our prior work and by others [1, 2, 4-6]. Therefore, the *Tie1* or *Tek* alleles were inactivated prior to the onset of atrial and ventricular trabeculations, as shown in Fig. 1, Fig. 2, Fig. 3, Fig. 5A-D, and Supplemental Fig. 3. Based on these findings, we propose that TIE1 is differentially required for atria versus ventricle morphogenesis, and acts synergistically with TIE2 during cardiac trabeculation.

> ***Public Reviews:***
>
> ***Reviewer #1 (Public review):***
>
> *Summary:*

> *In this manuscript, Ding et al. use genetic mouse models to demonstrate that atrial trabeculation is more dependent on Tie1/Tie2 signaling than ventricular trabeculation. With additional experimentation that would support the current claims, the results may hold significant value, as atrial trabeculation remains an understudied phenomenon in cardiac biology with potential implications for atrial cardiomyopathy and atrial fibrillation.*
>
> *Strengths:*
>
> *Detailed characterization of atrial versus ventricular trabeculation across different developmental timepoints, and the use of appropriate animal models to address the scientific question at hand.*
>
> *Weaknesses:*
>
> *The authors have consistently treated mice with tamoxifen after ventricular, but not atrial, trabeculation has already started. As such, the observed cardiac phenotypes - where predominantly atrial trabeculation is affected - might be a mere consequence of the precise time window in which Tie1/2 signaling was impaired, rather than a direct measurement of its relative importance for atrial versus ventricular trabeculation. The conclusions of the paper may thus be significantly strengthened by depleting Tie1/2 signaling prior to the onset of ventricular trabeculation, as is done for atrial trabeculation.*

We thank the reviewer for the comments.

Regarding the timeline of gene deletion and tamoxifen treatment, we would like to provide the following clarification.

Fig. 1-3: As described in the Methods and Materials, $Tie1^{tm1a/tm1a}$ is a knockout first mouse model established from EUCOMM embryonic stem cells (EPD0735-3B07) targeting *Tie1* gene. Therefore, the $Tie1^{tm1a/tm1a}$ line is equivalent to the previously published *Tie1* null mice ($Tie1^{-/-}$). The $Tie1^{Flox/Flox}$ mouse line (with exon 8 floxed) was generated when the lacZ reporter and neo-cassette were excised using the FLPeR mice.

Fig. 5A-D: To investigate the synergy of TIE1 and TIE2 in cardiac trabeculation, we utilized the $Tek^{+/-}$ and $Tie1^{\Delta ICD/+}$ mouse lines and they were crossbred to generate double mutant mice harboring a homozygous *Tie1* mutation and a single null *Tek* allele ($Tie1^{\Delta ICD/\Delta ICD}$;$Tek^{+/-}$). Although no obvious defects were observed in atrial or ventricular structures following *Tie1* deficiency alone at E10.5, both atria and ventricle development were disrupted in $Tie1^{\Delta ICD/\Delta ICD}$;$Tek^{+/-}$ mutants at the same stage (Fig. 5A-D).

Supplemental Fig. 3: To verify the role of TIE1 in atrial development, we employed alternative knockout mouse line targeting the *Tie1* intracellular domain by floxing exons 15 and exon 16 ($Tie1ICD^{Flox/Flox}$). Mutants harboring these null alleles are designated as $Tie1^{\Delta ICD/\Delta ICD}$. As detailed in the previous publication [2], the line is also equivalent to the previously published *Tie1* null mice ($Tie1^{-/-}$). The cardiac phenotypes shown in Supplemental Fig. 3 are indeed similar to those of $Tie1^{tm1a/tm1a}$ mutant mice.

For the inducible knockouts targeting *Tie1*, *Tek* and both, the results are shown in Fig. 4, Fig. 5E-H, Fig. 6, Fig. 7.

Fig. 4: As mice homozygous for *Tek* mutation ($Tek^{-/-}$) die before E10.5 [3, 7], we performed studies using the inducible knockout line targeting *Tek* ($Tek^{Flox/-}$;$Cdh5\text{-}Cre^{ERT2}$ named as Tek^{iECKO}), as shown in Fig. 4.

Fig. 5-7: To investigate the synergy of TIE1 and TIE2 in the cardiac trabeculation at the later stages of embryogenesis (Fig. 5E-H, Fig. 6) and the postnatal stage (Fig. 7), we used the inducible knockout models targeting *Tie1/Tek*, including *Tie1ICD*^{iECKO} (*Tie1ICD*$^{Flox/-}$;*Cdh5-Cre*^{ERT2}) and *Tie1ICD*^{iECKO};*Tek*$^{+/-}$ (*Tie1ICD*$^{Flox/-}$;*Cdh5-Cre*^{ERT2};*Tek*$^{+/-}$).

> ***Reviewer #2 (Public review):***
>
> *Summary:*
>
> *Ding et al. examine the role of TIE1 in cardiac chamber morphogenesis using genetic mouse models targeting Tie1, Tek, or both, and analyzing endocardial cell-mediated chamber formation across multiple embryonic developmental and postnatal stages, supported by analysis of published single-cell datasets and new bulk RNA seq analyses of murine cardiac tissue. The authors find that Tie1 and Tek expression is higher in atrial than ventricular endocardial cells. Notably, endothelial Tie1 is required for atrial trabeculation at E12.5, but is less critical in ventricular trabeculation. TIE1 also acts synergistically with TIE2 during atrial trabeculation. While Tie1 deficiency alone does not cause defects at E10.5, combined heterozygous deletion of Tek disrupts both atrial and ventricular development at E10.5. This synergy is further supported by analyses at later embryonic stages and in postnatal hearts.*
>
> *Strengths:*
>
> *The study is well-designed, clearly written, and supported by high-quality figures. The performed experiments demonstrate a previously unrecognized role for Tie1 in cardiac development and identify synergistic control of cardiac morphogenesis by Tie1 and Tie2. This synergy is consistent with the previously identified roles of Tie1 and Tek in venous development and with Tie1 involvement in angiopoietin-dependent postnatal vascular and lymphatic remodeling. Together, these findings support a role for Tie1 as a contributor to Ang1-Tie2 signaling during heart development.*
>
> *Weaknesses:*
>
> *The manuscript does not include direct mechanistic studies; however, RNA seq analysis of atria and ventricles showed reduced expression of Tek, Dll1, and Notch1 upon Tie1 deficiency in developing hearts. Although previously reported mechanisms, such as TIE1-TIE2 heterodimer formation and effects on endothelial junctions, migration, or survival are discussed, no direct mechanistic experiments are performed. Addressing some of these mechanisms would have clarified the basis of Tie1-Tie2 synergy. As two distinct Tie1 models are used, including one targeting the kinase domain, the authors should state whether phenotypes differed or were similar between models.*

We thank the reviewer for the comments. In this study, we have provided genetic evidence that TIE1 is differentially required for atrial versus ventricular trabeculation. Although the precise molecular mechanisms underlying TIE1 function require further investigation, we have provided compelling genetic evidence of its synergistic role with TIE2 during this process. The two genetic models targeting *Tie1* (*Tie1*$^{tm1a/tm1a}$, *Tie1*$^{\Delta ICD/\Delta ICD}$) produced consistent cardiac and vascular phenotypes as shown in this study and our previous work [1, 2].

> ***Reviewer #3 (Public review):***
>
> *Summary:*
>
> *Ding et al. investigate the roles of TIE1 and TEK (Tie2) in mouse cardiac development, with a particular focus on atrial trabeculation. The authors employ multiple genetic*

models, including Tie1ICDflox/flox (with Cdh5-CreERT2), a knockout-first allele (EUCOMM, Tie1 tm1a/tm1a), and a Tek deletion model.

Based on the dataset from Feng et al. 2022 Nat Commun, the authors report increased expression of Tie1 and Tek transcripts in atrial endocardial cells compared to ventricular cells at embryonic day (E) 14.5. Loss of Tie1 leads to early atrial trabeculation defects detectable at E12.5, whereas ventricular defects appear later and are less pronounced at E14.5. Chamber-specific RNA sequencing reveals stronger transcriptional changes in atrial tissue.

Conditional deletion of Tek results in a similar phenotype, with more pronounced atrial defects. Combined deletion of Tie1 and Tek (Tie1 ΔICD/ΔICD; Tek+/-) leads to earlier and more severe defects in both atrial and ventricular trabeculation and results in embryonic lethality around E12.5, suggesting a synergistic interaction between the two genes.

Conditional endothelial deletion of Tie1 combined with heterozygous global Tek at later embryonic stages allows analysis at later time points and again shows more severe defects in atrial trabeculation. Postnatal analysis of this model reveals reduced heart-to-body weight ratios and potential mild atrial abnormalities.

Strengths:

(1) The authors address chamber-specific signaling mechanisms underlying atrial versus ventricular trabeculation, an area of high developmental and clinical relevance.

(2) The study provides a comprehensive temporal analysis across multiple embryonic stages.

(3) The use of multiple genetic models strengthens the overall conclusions and allows comparative interpretation.

(4) While focusing on trabeculation, the authors also include observations on coronary vessel development, increasing the broader relevance of the work. The findings are therefore of interest to the wider cardiovascular research community.

Weaknesses:

(1) Timing of recombination vs. trabeculation onset

Ventricular trabeculation begins earlier than atrial trabeculation. Since tamoxifen (in contrast to 4-hydroxytamoxifen) requires metabolic activation, Cre-mediated recombination will occur with a delay. This suggests that atrial trabeculation may be targeted before its onset, whereas ventricular trabeculation may already be underway for 2-3 days at the time of effective gene deletion.

How do the authors account for this discrepancy in their interpretation?

Have earlier induction time points been tested to better capture the onset of ventricular trabeculation? This limitation should be explicitly discussed.

(2) Clarity of genetic models and experimental design

The study employs several genetic constructs. It would improve clarity if, for each experiment, the specific genetic model and tamoxifen regimen were clearly described before presenting the results.

We thank the reviewer for the detailed and constructive comments. For studies employing the inducible gene deletion mouse models, the genetic models and tamoxifen treatment schemes have been provided in the related figures. For the rest of studies, we used the

conventional knockouts targeting *Tie1* and *Tek* (*Tie1*$^{tm1a/tm1a}$, *Tie1*$^{\Delta ICD/\Delta ICD}$ and *Tie1*$^{\Delta ICD/\Delta ICD}$;*Tek*$^{+/-}$), as detailed above.

> *(3) Tie1 tm1a/tm1a phenotype vs. known global knockout*
>
> *Previous studies (PMID: 8846781, 7596437) show that complete Tie1 loss leads to severe edema, vascular rupture, and embryonic lethality around E13.5-E14.5.*
>
> *How does the Tie1 tm1a/tm1a allele differ, given that animals appear to survive longer? Is this allele hypomorphic rather than a full knockout?*
>
> *This point requires clarification.*

Tie1$^{tm1a/tm1a}$ is equivalent to the full knockout (*Tie1*$^{-/-}$). As demonstrated in our prior work, the *Tie1*$^{\Delta ICD/\Delta ICD}$ model produced lymphatic and blood vascular phenotypes similar to those of *Tie1*$^{-/-}$ mutants [1, 2, 5, 6].

> *(4) Limited mechanistic insight*
>
> *While the authors aim to investigate underlying mechanisms, the current study is largely descriptive and based on mRNA expression and genetic interaction analyses (Tie1/Tek co-deletion). Direct mechanistic insights into signaling pathways remain limited. However, the dataset provides a valuable foundation for future mechanistic studies, which should be more clearly acknowledged in the discussion.*

We thank the reviewer for the comments. The manuscript will be revised accordingly, and a detailed response will be provided in our final submission.

Reference

(1) Cao, X., et al., Endothelial TIE1 Restricts Angiogenic Sprouting to Coordinate Vein Assembly in Synergy With Its Homologue TIE2. Arterioscler Thromb Vasc Biol, 2023. 43(8): p. e323-e338.

(2) Shen, B., et al., Genetic dissection of tie pathway in mouse lymphatic maturation and valve development. Arterioscler Thromb Vasc Biol, 2014. 34(6): p. 1221-30.

(3) Chu, M., et al., Angiopoietin receptor Tie2 is required for vein specification and maintenance via regulating COUP-TFII. Elife, 2016. 5:e21032.

(4) Rodewald, H.R. and T.N. Sato, Tie1, a receptor tyrosine kinase essential for vascular endothelial cell integrity, is not critical for the development of hematopoietic cells. Oncogene, 1996. 12(2): p. 397-404.

(5) D'Amico, G., et al., Loss of endothelial Tie1 receptor impairs lymphatic vessel development-brief report. Arterioscler Thromb Vasc Biol, 2010. 30(2): p. 207-9.

(6) Qu, X., et al., Abnormal embryonic lymphatic vessel development in Tie1 hypomorphic mice. Development, 2010. 137(8): p. 1285-95.

(7) Dumont, D.J., et al., Dominant-negative and targeted null mutations in the endothelial receptor tyrosine kinase, tek, reveal a critical role in vasculogenesis of the embryo. Genes Dev, 1994. 8(16): p. 1897-909.

https://doi.org/10.7554/eLife.111156.1.sa0